WP 3: New concrete crushing and separation methods and pretreatment

Task 2: Screening of the output fractions of the innovative crushing treatments

Authors: A. Gholizadeh Vayghan, M. Everaert, P. Nielsen, R. Snellings

Study accomplished as part of the Interreg Vlaanderen-Nederland project: Beton naar Hoogwaardig Beton

October 2020

VITO NV
Boeretang 200 - 2400 MOL - BELGIE
Tel. + 32 14 33 55 11 - Fax + 32 14 33 55 99
vito@vito.be - www.vito.be
BTW BE-0244.195.916 RPR (Turnhout)
Bank 375-1117354-90 ING
BE34 3751 1173 5490 - BBRUBEBB

DISTRIBUTION LIST

Hubert Rahier, VUB
Silviana Onisei, VUB
Michael El Kadi, VUB
Matilda Axelson, VUB
Jef Vleugels, KULeuven
Nicole Dilissen, KULeuven
Carlo Groffils, MEAM
Vincent Goovaerts MEAM
Simon Houtekier, CBS-Beton
Gert van der Wegen, SGS-Intron
Natalie Carr, SGS-Intron
Marc Steenbergen, ICDUBO
Asghar Gholizadeh Vayghan, VITO
Ruben Snellings, VITO
Peter Nielsen, VITO
Maarten Everaert, VITO
Mieke Quaghebeur, VITO

SUMMARY

Chapter 1 – Introduction: The main project goals are recited, the aim of the work package and the task activities are introduced.
Chapter 2 – Materials and methods: The materials delivered to and processed at VITO (if applicable) between the time span of March 2018 to March 2020, and the test methods used for their characterization/upcycling are laid out in Chapter 2.
Chapter 3 – Results: describes the original RCA properties and characterization results. Same is also provided for the processed batches of RCA each related to a specific treatment (i.e., SmartCrusher, GrondBank Nederland (ADR-HAS), microwaved RCA, and selective milling).
Chapter 4 – Discussion: makes a comparison between the different materials properties on a comparative basis to facilitate conclusions.
Chapter 5 – Conclusions and perspectives summarizes the conclusions by providing a factual list of main observations/take-aways followed by proposed next steps in the project (for further upscaling).

TABLE OF CONTENTS

LIST OF FIGURES

LIST OF TABLES

LIST OF ACRONYMS

RCA	Recycled concrete aggregates
RCF	Recycled concrete fines
RCCA	Recycled concrete coarse aggregates
RCFA	Recycled concrete fine aggregates
RAC	Recycled aggregate concrete
SCM	Supplementary cementitious materials
OPC	Ordinary portland cement
WA	Water absorption
SSD	Saturated surface dried
RH	Relative humidity
BnB	Beton naar hoogwaardig beton
HCP	Hardened cement paste
GBN	GrondBank Nederland
SCC	Smart Crusher Company

EXECUTIVE SUMMARY

Seven batches of materials were delivered to VITO between the 28/3/2018 and 28/2/2020 period in the form of raw concrete rubbles, crushed and processed recycled concrete fines and coarse aggregates. The **physical and mechanical properties of the virgin coarse and fine aggregates** used in the production of the recycled concrete (referred to as the production waste in the report) were characterized in the first step to have a basis for assessing and comparing the properties and performance of the recycled concrete fines and coarse aggregate outputs. The characterized properties primarily included **particle size distribution, fines content, density, water absorption, resistance against fragmentation and wear**.
The results suggested that the aggregates used in the production of the recycled concrete (referred to as production waste) had suitable particle size distribution, water absorption, and resistance against fragmentation and wear.

The **recycled concrete fines** produced by **SCC** were then investigated for their physical and mineralogical properties to assess the viability of the SCC lab prototype crushing machine in properly recycling the production waste. As such, the fines were characterized in terms of their 1) mass ratio compared to the throughput feed, 2) particle size distribution, and 3) hydrated cement paste content in different size fractions using the bound water method and the results were communicated within the consortium.
The results suggested that the crushed concrete aggregates produced by the SCC lab prototype included a **very high fines content (36% < 2mm)** which later is shown to be considerably higher than what is produced via other methods. It was also observed that despite the initial expectations, the **SCC lab prototype crushed the coarse limestone aggregates** as opposed to liberating them from the cement matrix. These findings and the following unsuccessful crushing campaigns convinced the consortium to find alternative solutions for effective recycling of concrete production waste. It was also observed that different size fractions of the fines contained **15 – 43% of hydrated cement paste (HCP) with increasing values for finer fractions**.

A **new method of measuring** the mass percentages of **different constituents** (i.e., HCP, limestone, sand) in different size fractions **of recycled concrete** fines was developed at VITO, referred to as the **phase decomposition method**. The method takes in the chemical composition, loss on ignition and density of the (milled) fractions and uses a regression method to determine the amount of each ingredient within each size fraction. The method was calibrated using 12 calibration mixtures with known compositions in order to boost the methods accuracy. A sensitivity analysis was also carried out to determine the effects of variations (i.e., measurement errors) in each oxide content, LOI or density on the prediction outcome of the method.
A **maximum of 8.5% error** was observed in the determination of HCP content when testing the calibrated method against all calibration mixtures' batching ratios, which was concluded to be **suitable**. The sensitivity analysis also showed that while variations (i.e., measurement errors) in oxides like Al_2O_3, Fe_2O_3, MgO and K_2O barely affect the model's outcome, **variations in CaO and LOI cause significant changes** (e.g., 2% error in each leads to 17% change in the HCP estimation output). It is concluded that the accurate measurement of these two parameters are critical in the accuracy of the model outcomes.

A batch of **concrete production waste** was delivered to VITO by **CBS Beton** in the form of rubbles (benchmark material). The delivered materials was crushed (600 kg) using a laboratory jaw crusher and separated into fine and coarse fractions. The physical and mechanical properties of both fractions were first investigated and compared to the standard limitations set forth by EN 12620 and EN 206-1. The HCP content was also traced in different size fractions of the recycled fines for finding the fractions with highest cement paste content.
The fines were then subjected to a line of research where **semi-auto grinding** at different milling energies and conditions was used to separate the HCP from the aggregates (i.e., sand and crushed limestone). The objective of this task was to **liberate the aggregates and recover the cement** for being used in a higher end application such as use as partial replacement for cement in new concrete. Over ten different milling conditions were examined and the optimal conditions were adopted for the next processing/characterization steps.
The results showed that using **jaw crusher** for crushing concrete also lead to the **crushing of the limestone similar to smart crusher**. However, a considerably **lower amount of fines** was produced by this method. The water absorption of both coarse and fine aggregates produced from the production waste were found to be high and the aggregates were thus deemed not ideal for fully replacing virgin aggregates in the production of new concrete. It was observed that the **HCP in different fractions varied from 35 – 60 m% with increasing values for finer fractions** (as per the bound water method). The optimal milling conditions for separation of HCP from aggregates (using a ball mill with a 30-cm drum) was found to be milling at 40 rpm for 6 min using 1.5-cm steel balls. The particle size distribution of the recycled fines after milling were compared to the same before milling and it was realized that the mass proportions of the coarser fractions (> 0.5 cm) are decreased while those of finer fractions are increased, which is an indication of selective milling of HCP.

Recycled concrete (production waste) rubbles were also **microwaved at MEAM** at two temperatures (**200 °C and 300 °C**) and delivered to VITO for further processing and characterization. The delivered raw and microwaved samples were first crushed following the pre-established crushing scheme and the particle size distribution of the outputs were measured and compared. The fine fractions were then subjected to further experimental and analytical work to determine the distribution of HCP across different fractions. The bound water and phase decomposition methods were also applied to the fine fractions to determine the HCP in each fraction. This was carried out for the raw and microwaved concrete rubbles (two temperatures: 200 and 280 °C) and the results were compared to one another. The fines of each of the three sources were then milled using the protocol developed in the previous phase and the same set of experiments (bound water, chemical composition, LOI and density) were repeated to explore the possible transportation of the HCP from coarser fractions to finer fractions so that the physical separation of the cement and aggregates is facilitated. The fragilization of the fines as a result of microwaving, and the efficiency of microwaving and milling on the degree of HCP separation was also investigated. The results were then communicated with the consortium in detail.
It was observed that **microwaving results in fragilization of the production waste**, evidenced by comparison of the particle size distributions of raw and microwaved materials after being exposed to the same crushing steps. The microwaved materials were found to crush into smaller pieces compared to the raw material, and the one microwaved at higher temperature was found to be the most fragile. The hydrated cement paste contents measured per the bound water and the phase decomposition method showed close agreement and also showed the positive impact of later on milling on the transportation of the HCP towards the finer fractions. While milling was found to result in enrichment of finer fractions with HCP, no considerable difference was found between the materials microwaved at 200 °C and 280 °C.

Another set of processed production waste aggregates comprising seven different materials processed at GBN using the ADR and HAS technologies was delivered to VITO for characterization.

The water absorption and resistance against fragmentation (only for coarse material) was measured and the results were communicated with the consortium. The HCP contented were also tracked and traced using the bound water and the chemical phase decomposition method and the consortium was advised according to the results.
The water absorption results of both fine and coarse fractions (output of ADR and HAS technology) was found to be excessively large and considerably larger than the same fractions produced by using the jaw crusher. This was at first speculated to be due to higher HCP content. However, the bound water content measurements and chemical composition analyses both suggested that the fine and coarse fractions of the production waste processed with ADR/HAS technologies are very low and overall the results were found to be inconclusive.

CHAPTER 1 INTRODUCTION

The BnB project aims at developing and upscaling innovative concrete recycling technologies. In a first step the concrete considered is production waste from CBS-Beton. This concrete is a high durability concrete consisting of limestone aggregates, sand, Portland cement and slag. The production waste, or particular size fractions, was treated by SCC (smart crushing technology), MEAM (microwave heating) and GBN (ADR-HAS technology). The main aim is to reuse the treatment output fractions in new performant concrete products. Depending on their properties the recovered materials are used as binder constituent, filler, fine or coarse aggregate.

Within the BnB project, WP3 aims to test and optimize the innovative concrete crushing, microwaving and separation technologies. WP3 also delivers materials for binder and concrete development to the respective follow-up WPs. The performance of the innovative concrete recycling technologies is evaluated by measuring the proportions and properties of the output fractions. Within WP3, task 3.2 therefore deals with screening the characteristics of the aggregate fractions obtained by the concrete recycling test campaigns. This report describes the physical, chemical and mechanical properties of crushed concrete aggregates delivered to VITO either by CBS Beton, Smart Crusher, MEAM, or GBN. The materials are characterized for their technical merits for being used as partial or full replacement of virgin aggregates in making new concrete. As such, the physical properties such as water absorption, porosity, and density, chemical composition and hardened cement paste content and mechanical properties namely resistance against fragmentation, and resistance against wearing are monitored for the delivered materials. These activities mainly pertain to the recycled concrete coarse aggregates (RCCA). The feed material is always crushed concrete rubbles which is crushed via different ways (e.g., using smart crusher, laboratory jaw crusher with and without microwaving as a preprocessing step, or ADR-HAS technology offered by GBN).

In addition, a multi-faceted attempt is made among different partners to valorize the recycled concrete fines (RCF) as a binder constituent, either as supplementary cementitious material (SCM) combined with Portland cement, or as precursor for an alkali-activated binder. The higher hardened cement paste (HCP) content of this fraction could engender binding properties. However, since the HCP is interlocked with fine aggregates of the original concrete (i.e., siliceous sand), attempts such as selective milling have been made to further separate the hardened cement paste from the sand, thus increasing the purity and value of the processed RCF.

In summary, the work carried out within task 3.2 with respect to RCCA and RCF revolved around valorization, reuse and upcycling of different fractions of end-of-life or demolished concrete by trying to assess the viability of different innovative concrete waste recycling technologies applied by other partners or by the pre/post treatments developed at VITO.

CHAPTER 2 MATERIALS AND METHODS

The materials delivered to VITO were either in the form of concrete rubbles (i.e., from fine particles to hand-sized pieces), granulated concrete aggregates, or concrete constituents (i.e., fresh cement, sand, limestone, etc). The following section is a brief explanation of all materials delivered to VITO with applicable pre-/post-processing steps taken to further valorize the materials (if applicable).

2.1. MATERIALS

A list of materials received is provided in Table 1. The 1st round of reference materials was delivered by CBS Beton early on in the beginning of the project. The 2nd batch of material was concrete aggregates crushed by SCC and sent to VITO for characterization. The 3rd and 4th rounds were also produced during crushing campaigns at SCC and sent to VITO for assessment.

The 5th batch of materials was a 1.5 tonne sac of concrete rubbles supplied by CBS Beton directly. This batch was crushed at VITO (600 kg) using a laboratory jaw crusher by passing the rubbles through the crusher once at 15 mm opening and once at 8 mm opening. The resulting materials were then sieved on sieve size 3 mm and the materials were labeled as ASG/19460 (RCCA) and ASG/19461 (RCFA). The latter was sent to VUB for further characterization and valorization as binder constituent. Several experiments were also carried out on the same at VITO.

The 6th batch of material was processed and sent to VITO by MEAM, which included one 25-kg sample of CBS concrete rubbles with no preprocessing; one 25-kg of CBS concrete microwaved at 200 °C and one of the same quantity microwaved at 280-300 °C. The aim of microwaving was to see the effects of thermal treatment on potential weakening of the interfacial transition zone (i.e., the contact) between the aggregates and the hydrated cemenet paste (HCP). VITO also applied further crushing on the as-received materials (rubbles) to convert them into concrete aggregate size materials and simultaneously investigate whether microwaving affects the crushing performance of RCA. 3 rounds of crushing were applied; a 1st one at 15 mm opening, a 2nd at 10 mm opening and a 3rd at 7.5 mm opening. Further analyses are also executed to trace and determine the amount of HCP in each fraction of the RCA by VITO.

The 7th batch of materials delivered to VITO was primarily the output of the ADR-HAS treatment by GBN. The ADR-HAS treatment involves classification of concrete rubble according to particle size and material density. In a first step the Advanced Dry Recovery (ADR) unit is used to project concrete rubble horizontally by a rotor drum, the travel distance of the projected particles is used for classification. The recovered coarse fraction (4/8) is intended to be reused as RCA as is, the fine fractions (0/1; 1/4) are processed by the HAS thermal treatment unit to further separate sand and HCP and decompose wood and plastic impurities. The HAS unit operates at 600 °C using combustion of natural gas. Within the BnB the feasibility of substituting the HAS treatment by microwaving is studied.

Table 1. The list of materials delivered to VITO

Material batch	Material description	VITO internal code	Date received	Delivered by
1	Kalkmeel (Limestone powder) CBS-beton	ASG/18099	3/28/2018	**CBS Beton**
	Gewassen zeezand (siliceous sea sand 0/3) CBS-Beton	ASG/18098	3/28/2018	
	Gemalen en gegranuleerde hoogovenslak	ASG/18097	3/28/2018	
	CEM 1 52.5 R	ASG/18096	3/28/2018	
	Fijn granulaat CBS-Beton (Fine limestone: 2/6)	ASG/18095	3/28/2018	
	Grof granulaat CBS-Beton (Coarse limestone: 6/14)	ASG/18094	3/28/2018	
2	Gebroken beton (SCC)	ASG/18315	12/4/2018	**SCC**
	Gebroken beton (SCC) <2mm. Gedroogd bij 110°C voor breken.	ASG/18313	12/4/2018	
3	Gebroken nat betonmateriaal CBS 4-10mm 5/11/2018	ASG/18337	12/11/2018	**SCC**
	Gebroken nat betonmateriaal CBS 0-4mm 5/11/2018 slow milled DRIED AT 40°C	ASG/18336	12/11/2018	
	Gebroken nat betonmateriaal CBS 0-4mm 5/11/2018 3e batch DRIED AT 40°C	ASG/18335	12/11/2018	
	Gebroken nat betonmateriaal CBS 0-4mm 5/11/2018	ASG/18334	12/11/2018	
	SCC Gebroken <40mm juni 2018 DRIED AT 40°C	ASG/18333	12/11/2018	
	Gebroken droog betonmateriaal CBS >10mm 19/11/2018 ALREADY DRY	ASG/18332	12/11/2018	
	Gebroken nat betonmateriaal CBS >10mm 19/11/2018 DRIED AT 40°C	ASG/18331	12/11/2018	
	Gebroken droog betonmateriaal CBS 2-10mm 19/11/2018 (1.5 week at 110°C)	ASG/18330	12/11/2018	
	Gebroken nat betonmateriaal CBS 2-10mm 19/11/2018 DRIED AT 40°C	ASG/18329	12/11/2018	

Material batch	Material description	VITO internal code	Date received	Delivered by
4	SCC gebroken <40 mm: the <4mm fraction	ASG/19231	7/4/2019	**SCC**
	SCC gebroken <40 mm: the 4-10mm fraction	ASG/19230	7/4/2019	
	SCC gebroken <40 mm: the 10-22.4mm fraction	ASG/19229	7/4/2019	
	SCC gebroken <40 mm: the 22.4-40mm fraction	ASG/19228	7/4/2019	
5	CBS Concrete 2nd batch (Recipe 1) recycled fine aggregate	ASG/19461	11/24/2019	**CBS Beton**
	CBS Concrete 2nd batch (Recipe 1) recycled coarse aggregate	ASG/19460	11/24/2019	
6	Recycled Concrete Aggregates: Original Untreated	ASG/19476	12/11/2019	**MEAM**
	Recycled Concrete Aggregates: MW treated +/-200°C	ASG/19475	12/11/2019	
	Recycled Concrete Aggregates: MW treated 280-300°C	ASG/19474	12/11/2019	
7	GBN Coarse 4/8_ADR	ASG/19489	12/23/2019	**MEAM/GBN**
	GBN 1/4_HAS	ASG/19490	12/23/2019	
	GBN 0/1_ADR	ASG/19491	12/23/2019	
	GBN 0/1 HAS	ASG/19492	12/23/2019	
	MEAM-GBN 0/1_HAS	ASG/19493	12/23/2019	
	0/4 Airknives Microwaved at ~250 °C	ASG/20079	28/02/2020	
	0/1 Rotor Microwaved at ~220-250 °C	ASG/20080	28/02/2020	

2.2. METHODS

2.2.1. SAMPLE PRETREATMENT

The concrete materials, if received in the form of rubbles (which was the case in the 5th and 6th batch of materials received per Table 1), were crushed using a laboratory jaw crusher at VITO in steps in order to convert them into proper size RCA for further testing and characterisation. Figure 1 shows the flowchart of RCA production at VITO using the jaw crusher. The CBS concrete rubbles received in November 2019 were crushed in two steps; one pass through the crusher with opening set at 15 mm and once at 8 mm. The results of particle size distribution by sieve analysis are shown and discussed in the next chapter. The rubbles received from MEAM (6th batch) were crushed in three steps (16 mm, 10 mm and 7.5 mm) to produce more fines, which were then analyzed (chemically and physically) to investigate the effects of microwaving.

Figure 1. Sample pretreatment steps (left: concrete rubbles; mid-left: laboratory jaw crusher; mid-right: crushed material; right top and bottom: RCF and RCCA, respectively)

2.2.2. PARTICLE SIZE DISTRIBUTION (SIEVE ANALYSIS)

Particle size distribution of the RCA was determined via sieve analysis according to BS EN 933-1 [1] using the standard sieves as shown below:
Fines: Pan, 0.063mm, 0.125mm, 0.25mm, 0.5mm, 1mm, 2mm, 4mm
Coarses: Pan, 4 mm, 6.3mm, 8mm, 10mm, 12.5mm, 14mm, 16mm, 20mm

The objective of the sieve analysis was to determine the particle size distribution of coarse and fine aggregates. A continuous gradation (i.e., having proper amounts of aggregates on all different sizes) promotes a concrete with superior properties in both fresh and hardened states.

2.2.3. PARTICLE DENSITY AND WATER ABSORPTION MEASUREMENT

The objective of this test was to determine two important physical characteristics of RCA which are not only useful in determining the mixture design of new concrete, but also the suitability of RCA for use in new concrete. RCA with excessively high water absorption results in a drop and loss in concrete slump and shrinkage cracking later on in the setting stages.
These two tests are consecutive in the sense that once the particle density test is done, the water absorption will be measured after a simple step.

Particle density is calculated from the ratio of mass to volume. The mass is determined by weighing the test portion in the saturated and surface-dried condition and again in the oven-dried condition. The volume is determined from the mass of the water displaced, either by mass reduction in the wire basket method or by weighing in the pycnometer method. Both tests are performed differently for RCF and RCCA. Details of the test method are laid out in BS EN 1097-6 [2].

2.2.4. RESISTANCE TO FRAGMENTATION

The resistance of RCCA against fragmentation is one of the major control parameters that is measured per EN 1097-2 (Los Angeles test [3]) in which the weight percentage of RCA fragmented during the test is measured and reported as the Los Angeles factor (LA factor). A schematic diagram of the test is presented in Figure 2.
A 5000 g sample of slag (10-14 mm) is placed in the LA machine (Macben Model A4.1 conforming to EN 1097-2 specifications) with 11 steel balls with diameter ranging from 45 to 49 mm. After 500 revolutions at 31-33 rpm, the material is sieved at 1.6 mm and the percentage of material below is reported as the LA factor.

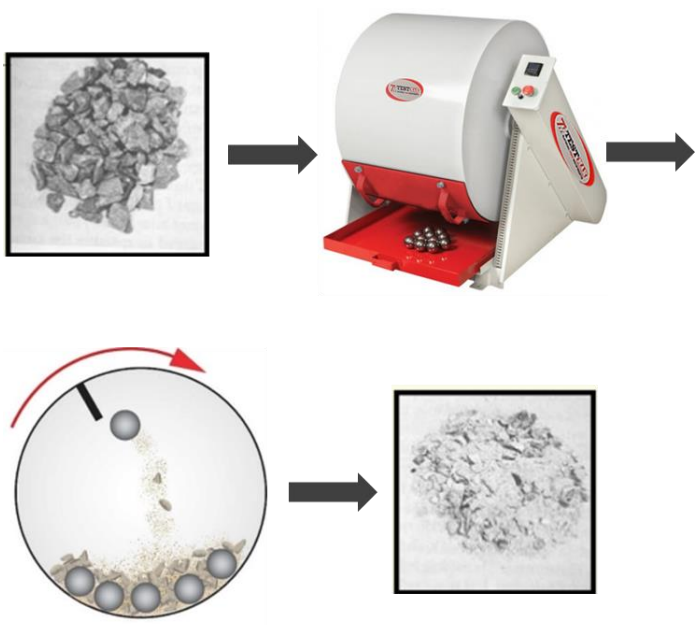

Figure 2. A schematic diagram of the Los Angeles test

2.2.5. RESISTANCE TO WEAR

The resistance of aggregates against wear is a recently regulated parameter that is measured per EN 1097-1 (micro-Deval factor [4]); in which the weight percentage of aggregates worn out during the test is measured and reported as the micro-Deval factor (MDE factor). A schematic diagram of the test is presented in Figure 3.
A 500 g sample of slag (10-14 mm) is placed in the MDE machine drum (Macben Model A077-01 conforming to EN 1097-1 specifications) with 2.5 L water and 5000 g of steel balls (diameter 10±0.5 mm). After 12,000 revolutions at 100 rpm, the MDE factor is reported as the fraction which passes a 1.6 mm sieve.

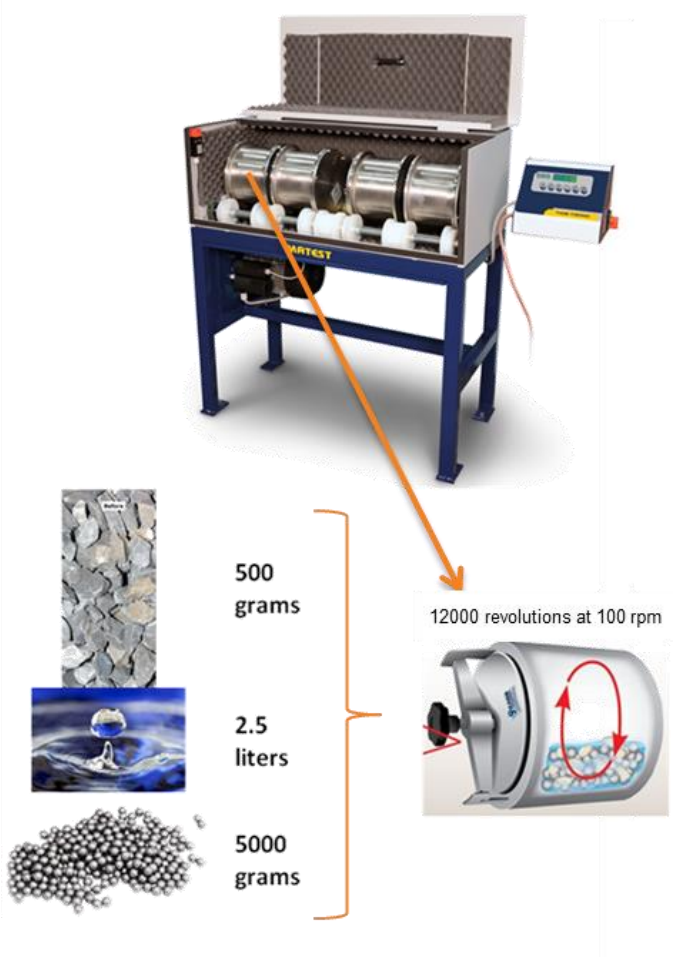

Figure 3. A schematic diagram of the micro-Deval test

2.2.6. ENERGY DISPERSIVE XRF ANALYSIS

Pulverized samples were analyzed using a high performance energy dispersive XRF spectrometer with polarized X-ray excitation geometry (HE XEPOS, Spectro Analytical Systems, Kleve, Germany). The instrument was equipped with a 50 W tungsten end window tube (max. 60 kV, 2 mA) and a Silicon Drift Detector. For signal optimization, different targets were applied. In Table 2, the applied measurement conditions are defined for loose powder analyses. All analyses were performed under He atmosphere. An XRF sampling cup, provided with a 4 µm prolene foil (Chemplex), was filled with the sample and subsequently, placed in the autosampler of the EDXRF system. The quantification was performed using a precalibrated software package.

Table 2. EDXRF measurement conditions for analysis as loose powder

Target	Tube conditions*	Measurement time
Compton, secondary, Molybdenum	40 kV, 1m A	500 s
Barkla scatter, Aluminium oxide	60 kV, 0.66 mA	600 s
Secondary (K), Cobalt	25 kV, 16 mA	500 s
Secondary (L), Palladium	20 kV, 2 mA	300 s

*With automatic current regulation

2.2.7. HELIUM PYCNOMETRY

The true density was measured, when applicable, using AccuPyc II 1340 V1.09 Helium phcnometer. 1-3 g of sample was placed inside the instrument chamber at ambient temperature and the chamber (volume 3.5 cm^3) was purged with Helium 10 times in order to eliminate all atmosphere, and the density was calculated by dividing sample mass (measured to the closest 0.00005 g) with its volume (measured to the closest 0.00005 cm^3).

2.2.8. DETERMINATION OF HYDRATED CEMENT PASTE CONTENT

Besides the use of RCCA as aggregate in new concrete, valorization of RCFA as SCM offers a wealth of benefits in making new concrete including a reduction in clinker content, reduction in heat of hydration, etc. As such VUB and VITO have been actively investigating the possibility of converting RCFA to a viable source of SCM. Since it is only the HCP portion of RCFA that might contribute to strength development (along with some contribution from calcium carbonate), it is important to trace the distribution of HCP in different size fractions of RCFA and also activate it by means of thermal heating or mechanical grinding. However, the first step is to determine the HCP content in the RCFA as a whole and also in each size fraction. To this end, two methods are applied, namely bound water measurement and phase decomposition. Below these methods are explained separately.

→ Bound water method for estimation of hydrated cement paste content in RCFA

In this method, the raw RCFA is sieved using the standard sieves introduced in section 2.2.2. Samples from each sieve are taken, heated at 40 °C for 24 hours, and pulverized using a high-impact ball mill at 400 rpm for a total of 5 minutes (final size < 125 µm). Next, representative specimens are taken and poured into porcelain crucibles and heated up to 550 °C inside an oven. Assuming a bound water content of 0.21 for the hydrated cement paste, the mass ratio of the hydrated cement paste is estimated by measuring the mass loss of the specimens in different size fractions. The formula for calculation of HCP content (in mass percent of the total RCF in dried state) is driven in the following

$$HCP\ (\%) = \frac{M_{HCP}}{M_{RCF.dry}} \times 100\%$$

$$M_{HCP} = M_{cem.} + M_{B.W.}[= 0.21M_{cem.}] = 1.21M_{cem.}$$

$$M_{RCF.dry} - M_{RCF.550°C} = M_{B.W.} = 0.21M_{cem.}$$

$$M_{HCP} = 1.21M_{cem.}[= \frac{M_{RCF.dry} - M_{RCF.550°C}}{0.21}] = 5.76\Delta M$$

$$HCP\ (\%) = 5.76\frac{\Delta M}{M_{RCF.dry}} \times 100\% \qquad \textit{(Equation 1)}$$

Where HCP (%) is the hydrated cement paste content (%), M_{HCP}, $M_{cem.}$, $M_{B.W.}$, $M_{RCF.dry}$ and $M_{RCF.ign.}$ are the masses of HCP, cement, bound water and RCF in dried and ignited states.

→ **Phase decomposition (target: tracing and determination of HCP content in each size fraction)**

Once the chemical composition, LOI content and density of each fraction was determined, the mass proportions of each constituting ingredient (i.e., hydrated cement paste, limestone and sand) was back calculated using a linear interpolation model by minimizing the sum of square differences between the observed and estimated 1- oxide contents, 2- LOI and 3- density, for each size fraction. The mathematics of this method is briefly explained below. Notice that for microwaved or thermally heated samples, the LOI and density values are uncontrollably affected by the thermal action and thus the below method will only rely on the chemical composition results in such cases.

If we consider cement paste, limestone and sand as the three main ingredients of each size fraction or output fraction of crushed concrete (RCA), and allow the dummy variable i to represent the ingredients, then:
i = 1 : Cement paste
i = 2 : Limestone (2/6 and 6/14)
i = 3 : Sand

Each ingredient has a set of fixed values for its oxide contents, LOI and density, all adding up vertically to the data vector of that ingredient. Therefore, the data vector of ingredient i will be:

$$\widetilde{D}_i = \begin{bmatrix} (CaO)_i \\ (SiO_2)_i \\ (Al_2O_3)_i \\ (Fe_2O_3)_i \\ (MgO)_i \\ (K_2O)i \\ (LOI)_i \\ \rho_i \end{bmatrix} \qquad \textit{(Equation 2)}$$

The XRF measurements suggest that for the CEM I 52,5R, Limestone 2/14, and sand 0/3; the combined data vector (=matrix) is:

$$\widetilde{D} = \begin{bmatrix} 44.0 & 42.25 & 5.09 \\ 14.7 & 15.6 & 85.8 \\ 4.82 & 2.105 & 2.04 \\ 2.02 & 0.407 & 0.912 \\ 1.55 & 1.355 & 0 \\ 0.26 & 0.15 & 0.653 \\ 24.70 & 36.17 & 4.46 \\ 2.302 & 2.7062 & 2.6689 \end{bmatrix}$$

The above grand data matrix is a fixed known for all output fractions. However, the mixing proportions of the three incredients (i.e., HCP: C, Limestone: L, and Sand: S) is variable in each output

fraction. As such, if we define the mixing proportions (MP) vector for the j^{th} output fraction as below:

$$\widetilde{\boldsymbol{MP}}_{\boldsymbol{j}} = \begin{bmatrix} \boldsymbol{C_j} \\ \boldsymbol{L_j} \\ \boldsymbol{S_j} \end{bmatrix} \qquad \textit{(Equation 3)}$$

The multiplication of $\widetilde{D}$ as a 7×3 matrix by $\widetilde{MP}_j$ yields a 7×1 vector that should be a close approximation of such output fraction (i.e., the j^{th} output fraction or $\widetilde{OF}_j$) if the C_i, L_j and S_j are properly estimated.

$$\widetilde{OF}_j = \begin{bmatrix} (CaO)_j \\ (SiO_2)_j \\ (Al_2O_3)_j \\ (Fe_2O_3)_j \\ (MgO)_j \\ (LOI)_j \\ \rho_j \end{bmatrix} \qquad \textit{(Equation 4)}$$

However, a random vector of error for each output fraction is inevitable (denoted as $\tilde{\varepsilon}_j$). Simply put, the below equation is valid for all output fractions. Since the method uses a realistic mathematical estimation of mass proportions of each ingredient using a linear model, the residuals vector $\tilde{\varepsilon}_j$ has a normal distribution with a mean of 0 and a variance of σ_j^2.

$$\widetilde{\boldsymbol{OF}}_{\boldsymbol{j}} = \boldsymbol{D} \times \widetilde{\boldsymbol{MP}}_{\boldsymbol{j}} + \tilde{\boldsymbol{\varepsilon}}_{\boldsymbol{j}} \qquad \textit{(Equation 5)}$$

Such formulation follows the same concepts as that of multiple (on dummy variable j) linear regression. Therefore, same is implemented using Minitab software to back calculate the mass proportions of the ingredients for different size fractions.

It can be shown that:

$$\widetilde{\boldsymbol{MP}}_{\boldsymbol{j}} = \left(\tilde{\boldsymbol{D}}^{\boldsymbol{T}}\tilde{\boldsymbol{D}}\right)^{-1}\tilde{\boldsymbol{D}}^{\boldsymbol{T}}\widetilde{\boldsymbol{OF}}_{\boldsymbol{j}} \qquad \textit{(Equation 6)}$$

$\rightarrow$ Calibration of the data vector ($\widetilde{D}$):

In order to assess the accuracy of the above method in estimating the mixing proportions of RCAs, a number of calibration mixtures with known proportions are produced and the mixing proportions are estimated using the developed method. Table 3 shows the mixing proportions of the calibration mixtures. The mixture proportions are chosen based on a simplex mixture design of experiments with a wide range of compositions. The cement paste content is assumed to range from 0.1–0.4, the limestone content from 0.2–0.6 and the sand content from 0.1–0.4 (see Figure 4). An extra mixture composing only cement and water is also produced and tested to improve the assessment.

Table 3. The mixture proportions of the calibration mixtures in ratios

Mix n°	HCP	Sand	Limestone
Mix01	0.1	0.4	0.5
Mix02	0.26	0.26	0.48
Mix03	0.33	0.33	0.34
Mix04	0.18	0.28	0.54
Mix05	0.1	0.3	0.6
Mix06	0.4	0.4	0.2
Mix07	0.3	0.1	0.6
Mix08	0.28	0.18	0.54
Mix09	0.33	0.18	0.49
Mix10	0.4	0.1	0.5
Mix11	0.18	0.33	0.49
Mix12	1	0	0

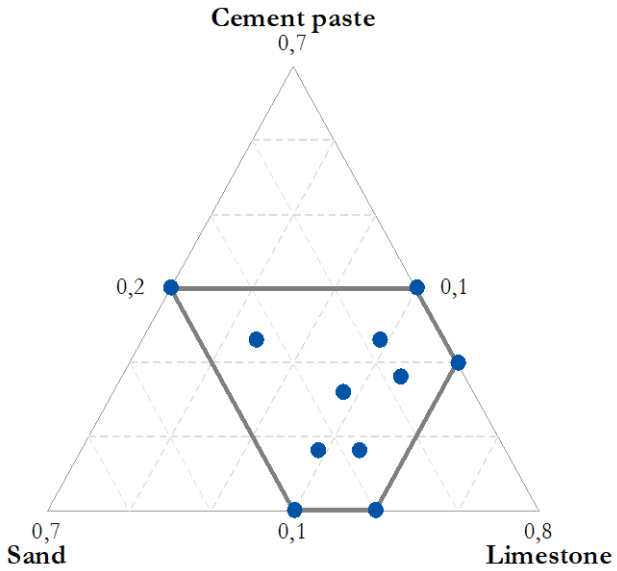

Figure 4. Simplex mixture design of experiments showing the studied ranges and the design data points

In order to produce the above mixtures with high accuracy, the aggregates (limestone and sand) are pulverized and blended in measured proportions with anhydrous cement powder. It is assumed that the cement absorbs 20% water (by mass) in order to turn into cement paste (for instance, 10 g of cement paste is composed of 8.33 g of cement and 1.67 g of water). Nonetheless, more water is added to the mixtures to promote plasticity and proper mixing. Table 4 shows the mixing proportions of the calibration mixtures in masses.

Table 4. The mixing proportions of the calibration mixtures in masses

Mix n°	Cement paste (g)	Cement powder (g)	Bound water (g)	Sand (g)	Limestone (g)	Water added (g)

Mix01	10	8.33	1.67	40	50	25.1
Mix02	26	21.67	4.33	26	48	25.2
Mix03	33	27.50	5.50	33	34	25.3
Mix04	18	15.00	3.00	28	54	25.4
Mix05	10	8.33	1.67	30	60	25.5
Mix06	40	33.33	6.67	40	20	25.3
Mix07	30	25.00	5.00	10	60	25.4
Mix08	28	23.33	4.67	18	54	25.1
Mix09	33	27.50	5.50	18	49	25.3
Mix10	40	33.33	6.67	10	50	25.3
Mix11	18	15.00	3.00	33	49	25.55
Mix12	100	83.33	16.67	0	0	36

The mixtures are then cured for 28 days and later dried at 40 °C to drive the extra water out. They are then crushed using a jaw crusher into small particles (<4 mm) and then pulverized using a planetary ball mill below 63 µm. The compositions, densities and LOI values of the mixtures are then measured using energy dispersive XRF and He pycnometry methods (see Table 5) and then used to estimate the predicted mixture proportions using the introduced method.

Table 5. The oxide composition, LOI and density of the calibration mixtures

Mix n°	CaO	SiO_2	Al_2O_3	Fe_2O_3	MgO	K_2O	LOI (%)	Density (g/cm^3)
Mix01	26.5	44.4	2.37	0.642	<1	0.413	22.77	2.6509
Mix02	33	33.9	2.97	0.914	1.17	0.433	25.21	2.5914
Mix03	31	38.1	3.14	1.04	1.13	0.462	22.72	2.5605
Mix04	31.2	35.8	2.71	0.764	1.11	0.407	25.73	2.623
Mix05	30.8	36.6	2.45	0.669	1.08	0.437	25.95	2.6546
Mix06	29.1	41.2	3.2	1.15	1.05	0.485	21.19	2.5296
Mix07	38.9	23.1	3.13	0.947	1.37	0.407	29.57	2.5812
Mix08	36.3	28	3.07	0.916	1.25	0.364	27.67	2.5863
Mix09	35.7	28.1	3.14	0.983	1.26	0.376	27.89	2.5661
Mix10	38.7	22.5	3.37	1.08	1.36	0.333	29.84	2.5408
Mix11	31.3	36.6	2.69	0.836	1.08	0.451	24.91	2.6212
Mix12	46.1	16.2	5.11	1.99	1.71	0.337	23.98	2.3021

The predicted values for the mixing proportions of cement paste (HCP), limestone and sand along with the original (batched) values and the prediction errors are presented in Table 6. It is observed from the last three columns that the prediction errors for HCP content in most cases falls below 10%. However, in three cases (Mix01, Mix04 and Mix05) the prediction error is greater than 10%. Moreover, the prediction errors are larger (compared to those of cement) for sand and especially limestone. This implies that if this method is applied to other mixtures with unknown mixture proportions, similar errors might occur in predicting the mixing proportions. As such, it is advisable to use the calibration mixtures data to calibrate the data vector ($\widetilde{D}$) such that the errors in predicting the mixing proportions (especially that of HCP) is minimized. The method will then be used with the calibrated data vector for determining the hydrated cement paste of RCA.

Table 6. The predicted mixing proportions, batched proportions and prediction errors of different ingredients for the calibration mixtures

Mix n°	Predicted			Batched			Prediction errors		
	HCP	Limestone	Sand	HCP	Limestone	Sand	HCP	Limestone	Sand
Mix01	0.52%	57.34%	41.24%	10%	50%	40%	9.48%	7.34%	1.24%
Mix02	24.33%	49.72%	26.31%	26%	48%	26%	1.67%	1.72%	0.31%
Mix03	30.39%	37.95%	32.30%	33%	34%	33%	2.61%	3.95%	0.70%
Mix04	9.14%	61.05%	29.07%	18%	54%	28%	8.86%	7.05%	1.07%
Mix05	4.38%	64.87%	30.12%	10%	60%	30%	5.62%	4.87%	0.12%
Mix06	30.08%	33.30%	36.82%	40%	20%	40%	9.92%	13.30%	3.18%
Mix07	29.59%	60.07%	10.94%	30%	60%	10%	0.41%	0.07%	0.94%
Mix08	27.10%	55.66%	17.88%	28%	54%	18%	0.90%	1.66%	0.12%
Mix09	22.36%	59.30%	18.15%	33%	49%	18%	10.64%	10.30%	0.15%
Mix10	27.42%	62.14%	10.24%	40%	50%	10%	12.58%	12.14%	0.24%
Mix11	15.44%	54.49%	30.11%	18%	49%	33%	2.56%	5.49%	2.89%
Mix12	117.96%	-14.12%	1.23%	100%	0%	0%	17.96%	14.12%	1.23%

The calibration of the data vector ($\widetilde{D}$) means finding values for its arrays slightly different than what the XRF, LOI and He pycnometry methods measured (by 15%, 5% and 15%, respectively) in such a way that the prediction errors of the hydrated cement paste, limestone and sand is minimized across the 12 calibration mixtures. The calculations as per (Equation 6) yields the below (calibrated) data vector.

$$\widetilde{D}_{cal.} = \begin{bmatrix} 45.45 & 40.138 & 4.8355 \\ 15.393 & 14.82 & 81.51 \\ 5.0643 & 1.9998 & 1.938 \\ 2.1165 & 0.3867 & 0.8664 \\ 1.4763 & 1.4228 & 0 \\ 0.25 & 0.1575 & 0.6204 \\ 23.653 & 36.287 & 4.683 \\ 2.256 & 2.7603 & 5.5468 \end{bmatrix}$$

Using the above matrix, the predicted HCP, limestone and sand values for different mixtures is calculated and shown in Table 7. It is observed that the prediction errors for HCP content in almost all cases is below 9 m%, which is a good outcome given the complexity of the system.

Table 7. The predicted mixing proportions, batched proportions and prediction errors of different ingredients for the calibration mixtures after calibration

Mix n°	**Predicted**			**Batched**			**Absolute prediction errors (m%)**		
	HCP	**Limestone**	**Sand**	**HCP**	**Limestone**	**Sand**	**HCP**	**Limestone**	**Sand**
Mix01	8.15%	53.04%	44.52%	10%	50%	40%	1.85%	3.04%	4.52%
Mix02	28.00%	49.14%	28.32%	26%	48%	26%	2.00%	1.14%	2.32%
Mix03	32.29%	38.44%	34.72%	33%	34%	33%	0.71%	4.44%	1.72%

Mix04	15.73%	58.14%	31.38%	18%	54%	28%	2.27%	4.14%	3.38%
Mix05	12.00%	61.12%	32.54%	10%	60%	30%	2.00%	1.12%	2.54%
Mix06	31.60%	33.86%	39.57%	40%	20%	40%	8.40%	13.86%	0.43%
Mix07	33.33%	60.17%	11.77%	30%	60%	10%	3.33%	0.17%	1.77%
Mix08	30.86%	55.43%	19.24%	28%	54%	18%	2.86%	1.43%	1.24%
Mix09	26.93%	58.44%	19.56%	33%	49%	18%	6.07%	9.44%	1.56%
Mix10	31.45%	62.06%	11.03%	40%	50%	10%	8.55%	12.06%	1.03%
Mix11	20.74%	52.50%	32.46%	18%	49%	33%	2.74%	3.50%	0.54%
Mix12	103.81%	0.00%	0.75%	100%	0%	0%	3.81%	0.01%	0.74%

→ **Sensitivity analysis of the developed phase decomposition method**

In order to further assess the method's robustness in estimating the mixture proportions (especially the HCP content), a sensitivity analysis is carried out. The variations in the predicted HCP is quantified and plotted as a function of variations in the mixture parameters. To this end, the measured values of CaO, SiO_2, Al_2O_3, Fe_2O_3, MgO, K_2O, and LOI are varied (in 10% increments) from their originally measured values up to 100% in each direction (increase and decrease). The density is varied no more than +/-20% (in 2% increments) since it is quite unlikely for the helium pycnometry method to have larger errors. The changes in the HCP content is then calculated at each increment and plotted on a graph (results shown in Figure 5). It can be observed that variations in CaO and LOI are by far most influential in the estimation of HCP. A 2% error in the estimation of CaO or LOI leads to 17.6% and 14.8% relative change in the predicted HCP. As such, the measurement of these two parameters shall be carried out with ultimate care and a well-established protocol. The next influential parameter is Al_2O_3. 100% error in measurement of Al_2O_3 results in ~20% estimation error in HCP. The rest of the parameters were found to be of minimal influence.

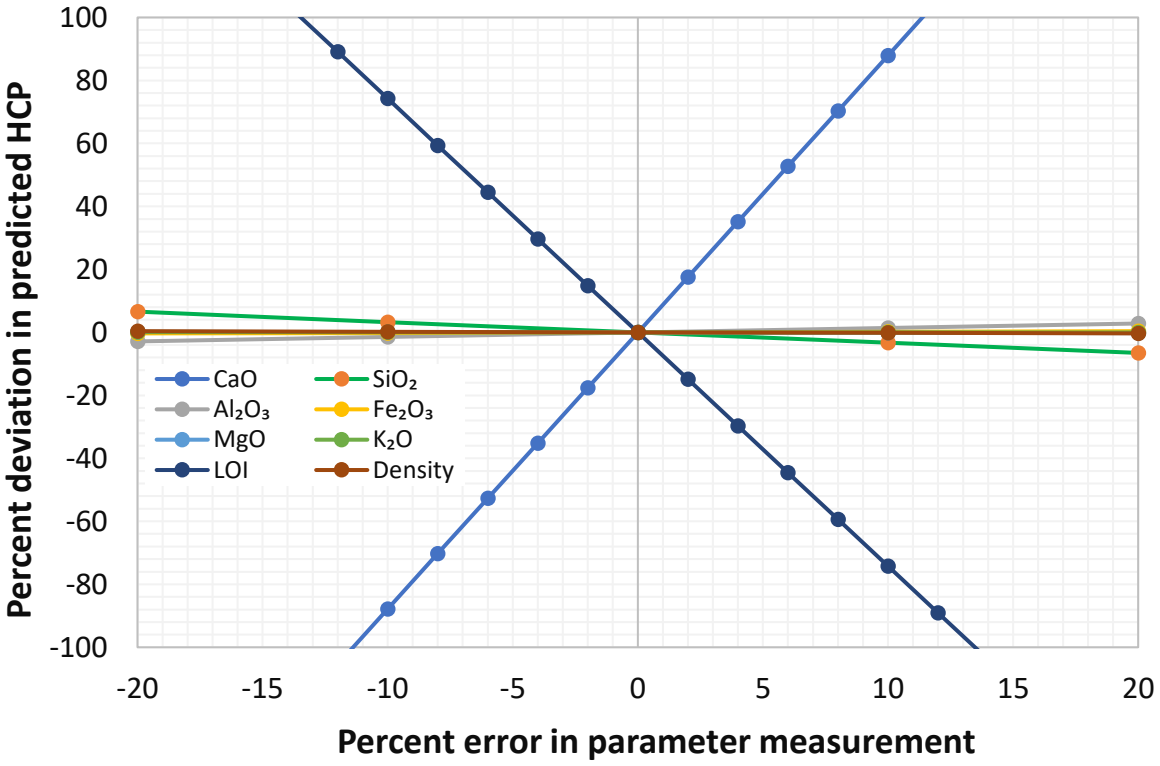

Figure 5. The variations in the estimated HCP content as a function of deviation in each mixture parameter (sensitivity analysis)

2.2.9. MILLING OF RCF FOR SAND RECOVERY (I.E., SEPARATION OF SAND AND HCP)

Selected RCF samples are milled using a 7-L ball mill (12 inches in diameter) at 40 rpm for 60 min using steel balls of diameter 1.5 mm with the aim of separating the aggregates (sand and limestone) from the cement and later sieving the pulverized cement for thermal reactivation and reuse as binder constituent in concrete.

CHAPTER 3 RESULTS

3.1. CHARACTERIZATION OF THE ORIGINAL CONCRETE INGREDIENTS

3.1.1. PHYSICAL PROPERTIES

Figure 6 shows the particle size distribution (sieve analysis) of the three sources of virgin aggregates used for making the reference concrete. The 6/14 fraction (i.e., the large size coarse aggregate) was also tested for resistance against fragmentation (i.e., Los Angeles test per 2.2.4) and was found to have an LA factor of 17.0%, which is well below the EN 206-1 [5] threshold of 50%. Figure 7 shows sample pictures of placing the aggregates in LA machine and the samples after the cycles of fragmentation.

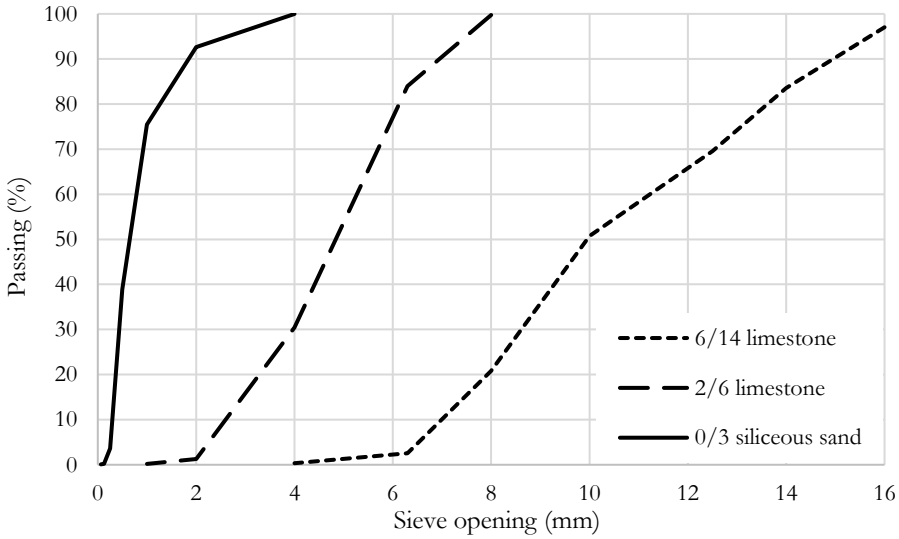

Figure 6. Particle size distribution results of the starting ingredients

Figure 7. Los Angeles testing steps. Left: placing the aggregates inside the machine's drum; Right: aggregates after the cycles of fragmentation

3.1.2. MECHANICAL PERFORMANCE

The resistance of the aggregates (both 2/6 and 6/14) against wear was measured per micro-Deval testing method (laid out in section 2.2.5). The results were found to be 14.9% and 16.1% for the two aggregates, respectively. Despite the fact that EN 206-1 does not specify a limiting value for this parameter, it is worth noting that the aggregates both show a low (i.e., satisfying) wearing factor.

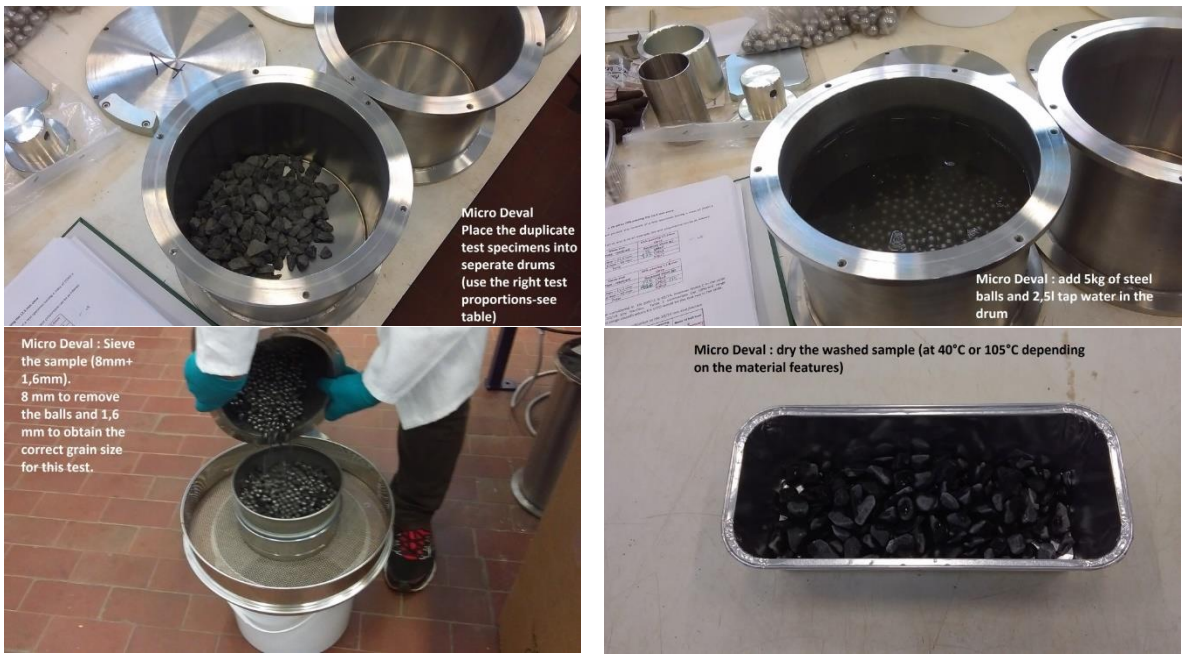

Figure 8. Micro-deval testing steps

3.2. CHARACTERIZATION OF THE RCA OUTPUT OF THE FIRST CRUSHING CAMPAIGNS OF SCC

3.2.1. PHYSICAL PROPERTIES

The first crushing campaign of CBS Concrete in SCC resulted in production of 59,065 kg of RCA with particle size ranging from 0 to 10 mm. The material was sieve separated at sieve size 2 mm and it was realized that the SCC treatment resulted in the formation of 36% of <2 mm materials (referred to as fines and labeled as ASG/18313) and 64% of >2 mm materials (coarses: ASG/18315). It is observed that in this trial SCC has produced a significant amount of fines, which was considered too much and thus not satisfactory. The particle size distribution of both above materials is shown in Figure 9.

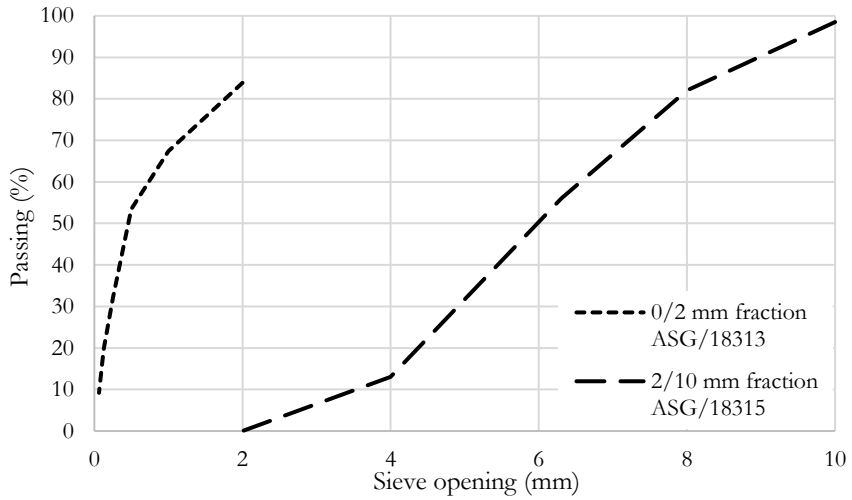

Figure 9. Particle size distribution of fine and corase fractions of CBS concrete crushed using smart crusher in the first crushing campaign.

3.2.2. DETERMINATION OF HYDRATED CEMENT PASTE CONTENT

The fines are investigated in terms of their mass loss as a function of temperature in order to trace their hydrated cement content (HCP). It is known that HCP loses all its bound water when heated up to 550 °C. Two samples were taken and tested for their loss on 550 °C (referred to as LOI). The HCP content was estimated using the bound water content under the assumption that a pure, fully hydrated HCP sample of CEM 52,5R contains 21% of bound water. Table 8 suggests that with reduction in particle size, the HCP content increases significantly, making the fraction a more suitable material for use as binder constituent. However, this is a preliminary result and requires further evaluation.

Table 8. The 550 °C mass loss (bound water) and approximate HCP content of different RCF fractions of CBS concrete crushed using the smart crusher (ASG/18313A)

Fraction (mm)	Specimen n°	Bound water measured	Calculated HCP content (%)	Average HCP content
>2 mm	1	2.9%	16.5	15.1±4.1%
>2 mm	2	2.4%	13.6	
1-2 mm	1	2.8%	15.9	15.8±0.3%
1-2 mm	2	2.7%	15.7	
0,5-1 mm	1	3.4%	19.5	19.3±0.7%
0,5-1 mm	2	3.3%	19	
0,25-0,5 mm	1	2.8%	16.4	16.4±0.1%
0,25-0,5 mm	2	2.8%	16.3	
0,125-0,25 mm	1	4.9%	28.4	28.2±0.6%
0,125-0,25 mm	2	4.9%	28	
0,063-0,125 mm	1	7.0%	40.6	40.2±1.1%
0,063-0,125 mm	2	6.9%	39.8	
< 0,063 mm	1	7.5%	43.3	42.8±1.6%
< 0,063 mm	2	7.3%	42.2	

3.3. CHARACTERIZATION OF THE RCA OUT OF THE SECOND AND THIRD CRUSHING CAMPAIGNS OF SCC

Due to the high fines content produced by the Smart Crusher (at SCC) in the subsequent second and thrid crushing campaigns, no further detailed experiments were carried out to characterize them (the materials listed in Table 9), as advised by the consortium and based on the initial findings.

Table 9. List of non-characterized materials

Material description	VITO internal code	Delivered by
Gebroken nat betonmateriaal CBS 4-10mm 5/11/2018	ASG/18337	SCC
Gebroken nat betonmateriaal CBS 0-4mm 5/11/2018 slow milled DRIED AT 40°C	ASG/18336	
Gebroken nat betonmateriaal CBS 0-4mm 5/11/2018 3e batch DRIED AT 40°C	ASG/18335	
Gebroken nat betonmateriaal CBS 0-4mm 5/11/2018	ASG/18334	
SB Gebroken <40mm juni 2018 DRIED AT 40°C	ASG/18333	
Gebroken droog betonmateriaal CBS >10mm 19/11/2018 ALREADY DRY	ASG/18332	
Gebroken nat betonmateriaal CBS >10mm 19/11/2018 DRIED AT 40°C	ASG/18331	
Gebroken droog betonmateriaal CBS 2-10mm 19/11/2018 (1.5 week at 110°C)	ASG/18330	
Gebroken nat betonmateriaal CBS 2-10mm 19/11/2018 DRIED AT 40°C	ASG/18329	
SCC gebroken <40: the <4mm fraction	ASG/19231	SCC
SCC gebroken <40: the 4-10mm fraction	ASG/19230	
SCC gebroken <40: the 10-22.4mm fraction	ASG/19229	
SCC gebroken <40: the 22.4-40mm fraction	ASG/19228	

3.4. CHARACTERIZATION OF THE CONCRETE RUBBLES SENT BY CBS BETON TO VITO

3.4.1. PHYSICAL PROPERTIES

A batch of production waste concrete rubbles was sent by CBS Beton to VITO and crushed using a regular lab jaw crusher. The coarse and fine fractions were separated at 4 mm. As such, 430 kg of coarse and 170 kg of fines were obtained. The fine content was thus 28.3% and the coarse content 71.7%. It is observed that the amount of fines is considerably smaller than that produced by Smart Crusher. Figure 1 shows the particle size distribution of the coarse and fine fractions.

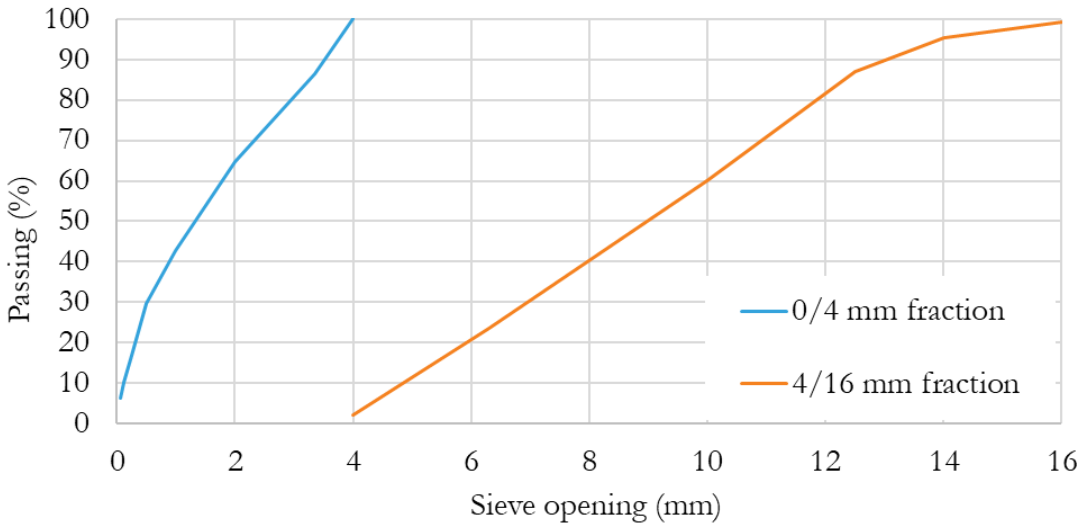

Figure 10. The particle size distribution of the coarse and fine fraction of RCA produced from CBS concrete rubbles using jaw crusher at VITO

3.4.2. MECHANICAL PROPERTIES

The LA factor and micro-Deval factor of this material was measured as 22.9% and 18.7%, respectively, which are satisfying and below EN 206-1 and other related standards thresholds.

3.4.3. WATER ABSORPTION

The water absorption of the coarse fraction is measured as 4.7%. This is slightly above normal and rather high for coarse aggregates. However, as a remedy RCCA can be soaked in water or wetted before use in making new concrete with no major issue. Similar strength values have been reported for normal strength concrete made with 25–30% replacement of aggregates with RCCA [6-8]. For the fine fraction (RCF), the water absorption is found to be 10.0%, which is too high (but a typical number found in other references as well [7, 9]). As such, the use of regular RCF as aggregate in new structural concrete is normally not recommended [10]. Instead, valorization of RCF cleaned from HCP could be used as aggregate. To this end, determination of HCP content is a good start to find out the potential value of the material and finding ways for its utilization.

3.4.4. HYDRATED CEMENT PASTE CONTENT

The estimation of the hydrated cement paste content on each fraction has been carried out for all size fractions of this material (both before and after milling) via the phase decomposition and bound water methods as laid out in the next section.

→ Phase decomposition method

The chemical compostition of different fractions was first measured via EDXRF method. Table 10 shows the oxide composition, LOI and density of different fractions of the RCF produced from CBS concrete. These results are analyzed using the phase decomposition method laid out earlier and the mass proportion of different ingredients for each size fraction is determined. Figure 11 shows the

phase decomposition analysis results. It is observed that the HCP content is constant for the first three fractions (i.e., in the 0.5 – 4 mm range) followed by a drop in the 0.25–0.5 mm and some increase in the finer fractions.

Table 10. Oxide composition of different size fractions of RCF from CBS concrete crushed using jaw crusher at VITO (ASG/19461)

	Size range (mm)						
Parameter	2 – 4	1 – 2	0.5 – 1	0.25 – 0.5	0.125 – 0.25	0.125 – 0.063	<0.063
CaO (%)	31.4	29.3	27.1	20.3	25.7	31.5	33.9
SiO_2 (%)	35.7	39.4	43.6	56	44.7	34.4	28.7
Al_2O_3 (%)	3.34	3.61	3.67	3.28	4.09	4.67	4.45
Fe_2O_3 (%)	0.7275	0.72	0.74	0.724	0.928	1.03	1.02
MgO (%)	1.625	1.6	1.6	1.31	1.72	2.11	2.11
K_2O (%)	0.3555	0.384	0.392	0.543	0.569	0.615	0.414
LOI (%)	24.36	22.53	20.57	15.74	19.80	22.94	26.52
Density (g/cm^3)	2.6753	2.6628	2.6399	2.6298	2.6615	2.6063	2.5871

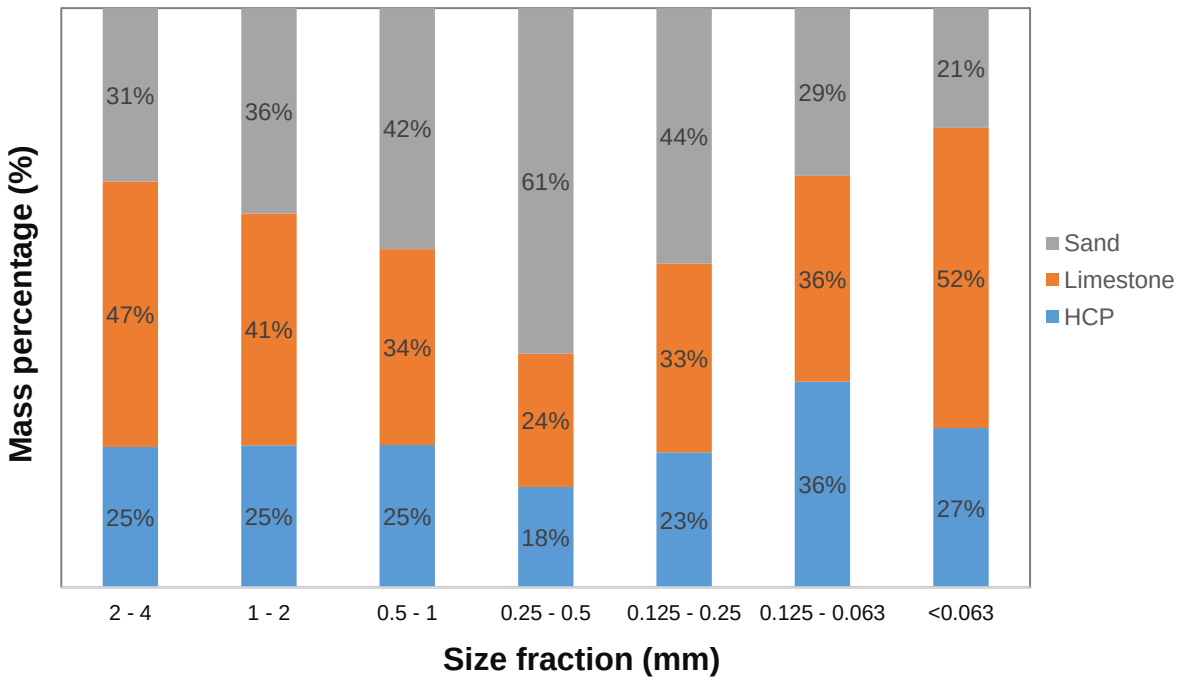

Figure 11. The barchart of mass proportions of ingredients in different size fraction of RCF (ASG/19461)

→ **Bound water method**

Table 11 shows the loss on ignition at 550 °C for different size fractions of CBS concrete's RCF. It is observed that the small fractions <1 mm are composed of at least 49-50% of HCP. Using mass balance it can be shown that ASG/19461 contains 44.94% HCP.

Table 11. The 550 °C mass loss (LOI) and approximate HCP content of different RCF fractions of CBS concrete crushed using jaw crusher at VITO (ASG/19461)

Fraction (mm)	Specimen n°	LOI at 550 °C	Approximate HCP content (%)	Average HCP content
<63 µm	1	9.70	55.88	55.88%
	2	–	–	
63-125 µm	1	9.92	57.15	57.15%
	2	–	–	
125-250 µm	1	9.66	55.67	61±15.1%
	2	11.52	66.37	
250-500 µm	1	9.29	53.51	55.2±4.8%
	2	9.87	56.88	
0.5-1 mm	1	8.18	47.09	53.9±19.3%
	2	10.55	60.76	
1-2 mm	1	6.05	34.82	36.9±6%
	2	6.78	39.04	
2-4 mm	1	6.04	34.77	36.6±5.1%
	2	7.14	34	

A comparison has been made between the bound water and the phase decomposition methods with regards to the HCP content (in %) and also in grams per each 100 grams of RCF. The results are provided in Table 12. It is observed that the methods have yielded rather different results leading to different total mass proportions of HCP (25.5 % for phase decomposition method compared to 44.94% for the bound water method). While an average of ~45% for HCP in the RCF seems to be too high considering the mixture design of the concrete, the estimated 25.5% also appears to be an underestimation.

Table 12. Comparison of the HCP (%) and HCP mass (g/100 g of RCF) between the phase decomposition and bound water methods for different size fractions of RCF from CBS concrete crushed using jaw crusher at VITO (ASG/19461)

		Size range (mm)							
Method	**Parameter**	2 – 4	1 – 2	0.5 – 1	0.25 – 0.5	0.125 – 0.25	0.063 – 0.125	< 0.063	**Sum**
	Retaining (%)	35.18	22.16	13.06	12.71	6.62	3.88	6.39	
Phase decomposition	HCP (%)	25.4%	26.0%	26.3%	19.4%	25.0%	37.0%	28.4%	
	Mass HCP (g/100 g RCF)	8.94	5.76	3.44	2.47	1.66	1.44	1.81	25.52
Bound water	HCP (%)	36.6%	36.9%	53.9%	55.2%	61.0%	57.2%	55.9%	
	Mass HCP (g/100 g RCF)	12.88	8.18	7.04	7.02	4.04	2.22	3.57	44.94

3.5. CHARACTERIZATION OF THE CONCRETE RUBBLES SENT BY MEAM TO VITO

In parallel to the concrete rubbles sent to VITO by CBS Beton (characterized in the previous section), another batch was sent to MEAM (referred to as RCA 0/40) for microwaving prior to crushing with the aim of weakening the HCP and facilitating the liberation of the aggregates during crushing. The RCA 0/40 was microwaved at two temperatures: 200 °C and 280-300 °C. A sample of each along with a sample of untreated (i.e., non-microwaved) RCA was sent to VITO from MEAM for crushing and characterization. Table 13 shows the list of materials sent to VITO along with a short description and the ASG codes. The characterization results are provided in the following sections.

Table 13. The list of materials sent by MEAM to VITO for crushing and chatacterization

Material description	ASG code
Untreated RCA 0/40	ASG/19476
RCA 0/40 MW 200°C	ASG/19475
RCA 0/40 MW 280-300 °C	ASG/19474

3.5.1. PHYSICAL PROPERTIES

The materials were crushed using the jaw crushing in three steps once at 15 mm opening, next at 10 mm opening and finally at 7.5 mm opening. Figure 12 shows the particle size distribution of the RCA after crushing. It is observed that microwaving results in the production of significantly finer RCA due to crushing (higher passing percentage at a given sieve size). The passing on 4 mm, for instance, which defines the amount of fines, is respectively 21%, 27.6% and 34.7% for the non-microwaved, microwaved at 200 °C and at ~290 °C. This suggests that the microwaving is effective in weakening the bond between the HCP and the aggregates of CBS concrete.

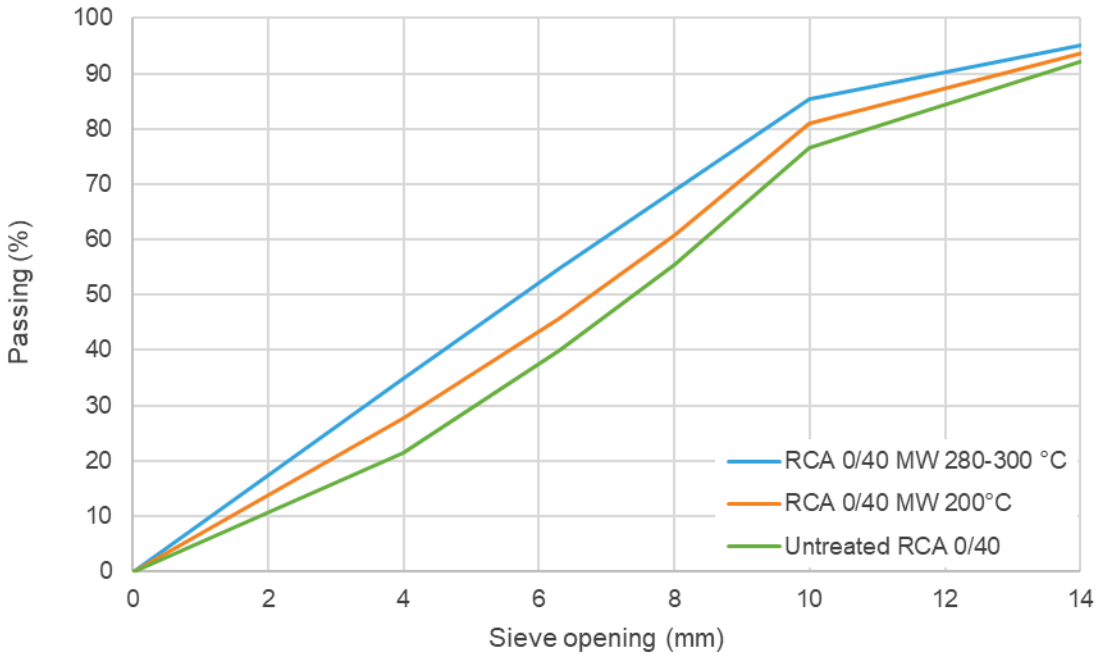

Figure 12. The particle size distribution of RCA sent by MEAM to VITO after crushing

3.5.2. MECHANICAL PERFORMANCE

The coarse fraction of all three materials are also tested for their resistance against fragmentation (LA test). The results are shown in Table 14. It is observed that the treated and raw RCAs have sufficient mechanical resistance (i.e., LA factor < 50% per EN 206-1) to be used in concrete as aggregates. The microwave treatment has slightly fragilized the RCA as shown by the slight increase in LA factor.

Table 14. Resistance against fragmentation (LA factor of raw and microwaved crushed RCA sent to VITO by MEAM

Material description	ASG code	LA factor (%)
Untreated RCA 0/40	ASG/19476	21.92
RCA 0/40 MW 200°C	ASG/19475	24.04
RCA 0/40 MW 280-300 °C	ASG/19474	23.88

3.5.3. WATER ABSORPTION

The results of water absorption of the fine RCF received from MEAM are shown in Table 15. It is observed that microwaving causes 6 – 8% increase in water absorption (depending on temperature) which could be due to resorption of water on dehydrated cement or shrinkage and formation of micro-cracks in the HCP structure or a combination of both. Nonetheless, the water absorption results are too high for application of the fines as fine aggregates in production of new concrete. However, unlike the non-microwaved RCF, the microwaved fines can be valorized as SCM and used in concrete as partial replacement for cement. This line of research has been pursued by VUB.

Table 15. Water absorption results of RCFs obtained through different processes

Untreated RCF	RCF MW 200°C	RCF MW 280-300 °C
ASG/19476	ASG/19475	ASG/19474
9.65	10.21	10.39

3.6. MILLING BEHAVIOR AND HYDRATED CEMENT PASTE CONTENT RESULTS

3.6.1. MILLING BEHAVIOR AND HCP CONTENT OF RAW RCA (ASG/19476)

All three materials are exposed to a milling process in order to investivate the efficiency of milling in separating the hydrated cement paste from the aggregates and transporting it to the finer fractions. Figure 13 shows the particle size distribution result of the raw RCA (i.e., ASG/19476) before and after milling via the procedure laid out in 2.2.9. The figure at the bottom shows the individual increases in the retained values on each sieve before and after milling. It is observed that milling has resulted in a decrease in the retained materials on the coarser sieves (above 0.5 mm) and a growing increase on the fine sieves (i.e., 0.25 mm and below). This is an indication of moderate milling of the material.

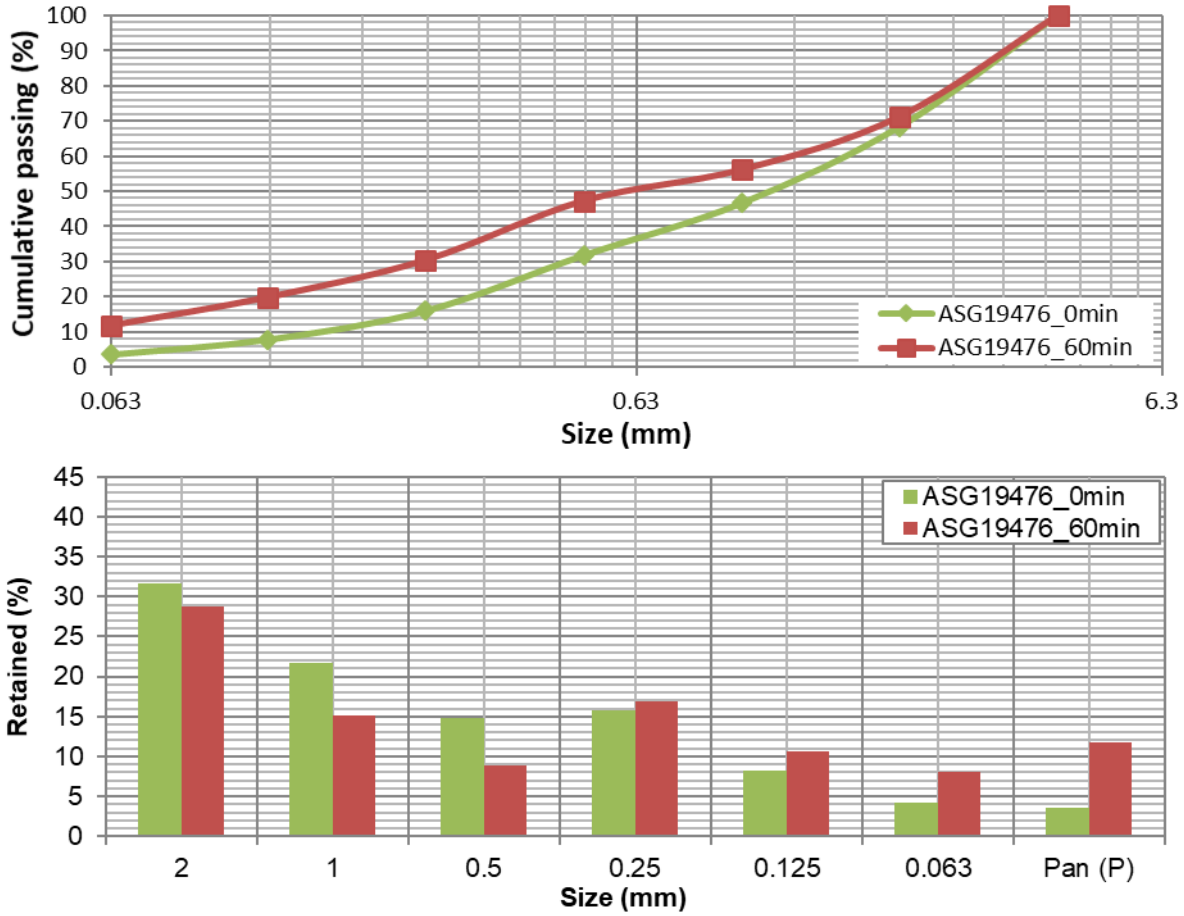

Figure 13. Particled size distribution change of raw RCF (19476) as a result of milling (top: cumulative passing; bottom: retained)

The estimation of the hydrated cement paste content on each fraction has been carried out for all size fractions of this material (both before and after milling) via the phase decomposition and bound water methods as laid out in the next section.

→ **Phase decomposition method**

The chemical composition of each fraction is measured and the HCP content on each fraction is estimated to trace the transportation of the most valuable ingredient (cement) due to milling to see whether milling of RCA (with and without microwaving) results in an improvement in the materials viability for being valorized as SCM. The oxide composition of different fractions is reported in Table 16. The phase decomposition method is applied on results to obtain the hydrated cement content in each fraction (see Figure 14). Similar to the case of RCF received from CBS, there is a drop in the HCP content for the 0.25–0.5 mm fraction, and that of finer fractions are higher. This trend is more pronounced for the same materials after milling (see Figure 14). The trend of variations in HCP, limestone, and sand is in line with the relative enrichment levels of the oxides such as CaO, Al_2O_3, and SiO_2. Figure 16 shows the relative enrichment levels of these three oxides. An enrichment in SiO_2 coupled with relative depletion of CaO and Al_2O_3 suggests the presence of more siliceous sand and less cement and limestone. Such trend is clearly visible both in Figure 14 and Figure 15. As such, the

phase decomposition method could be considered to be more reliable than the bound water method in this sense.

Table 16. Oxide composition of different size fractions of raw RCF received from MEAM (ASG/19476); before milling

	Size range (mm)						
Parameter	2 – 4	1 – 2	0.5 – 1	0.25 – 0.5	0.125 – 0.25	0.063 – 0.125	< 0.063
CaO	30.6	30	27	21.3	26.8	31.9	34.3
SiO2	38.3	39	43.6	55.5	44.4	33.4	28.9
Al2O3	3.53	3.65	3.65	3.39	4.11	4.71	4.62
Fe2O3	0.689	1.18	1.33	0.703	0.889	1.53	1.42
MgO	1.67	1.66	1.66	1.32	1.77	2.14	2.18
K2O	0.342	0.397	0.403	0.598	0.506	0.553	0.583
LOI(%)	22.54	21.47	20.31	15.84	19.88	22.61	24.89
Density	2.6753	2.6628	2.6399	2.6298	2.6615	2.6063	2.5871

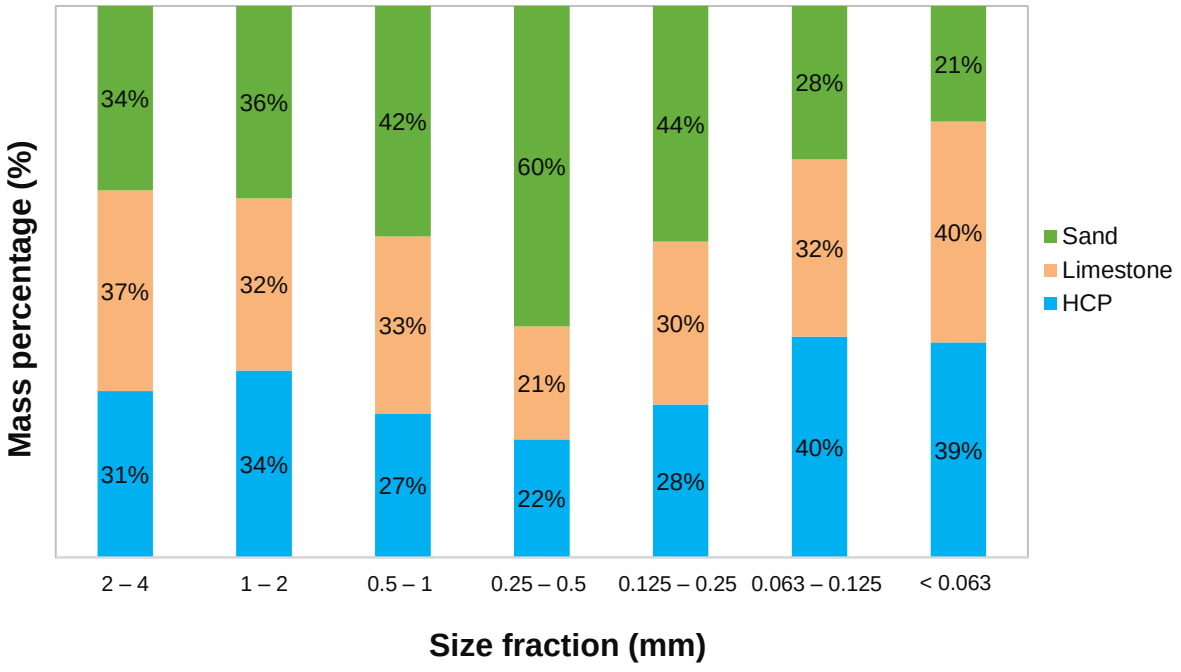

Figure 14. The barchart of mass proportions of ingredients in different size fraction of raw RCF received from MEAM (ASG/19476) before milling

Table 17. Oxide composition of different size fractions of raw RCF received from MEAM (ASG/19476); after milling

	Size range (mm)						
Parameter	2 – 4	1 – 2	0.5 – 1	0.25 – 0.5	0.125 – 0.25	0.063 – 0.125	< 0.063

CaO	30.7	31.2	29.2	17.1	21.9	30.6	35.3
SiO2	37.6	36.9	39.5	63.8	53.9	36.3	27.2
Al2O3	3.56	3.42	3.45	2.86	3.73	4.82	5.14
Fe2O3	1.01	1.19	0.701	0.58	1.54	1.66	1.08
MgO	1.69	1.57	1.56	1.02	1.39	2.16	2.42
K2O	0.36	0.338	0.43	0.53	0.596	0.516	0.486
LOI(%)	22.65	22.91	22.59	12.77	15.46	20.65	24.75
Density	2.6293	2.6549	2.6492	2.6469	2.6276	2.6407	2.592

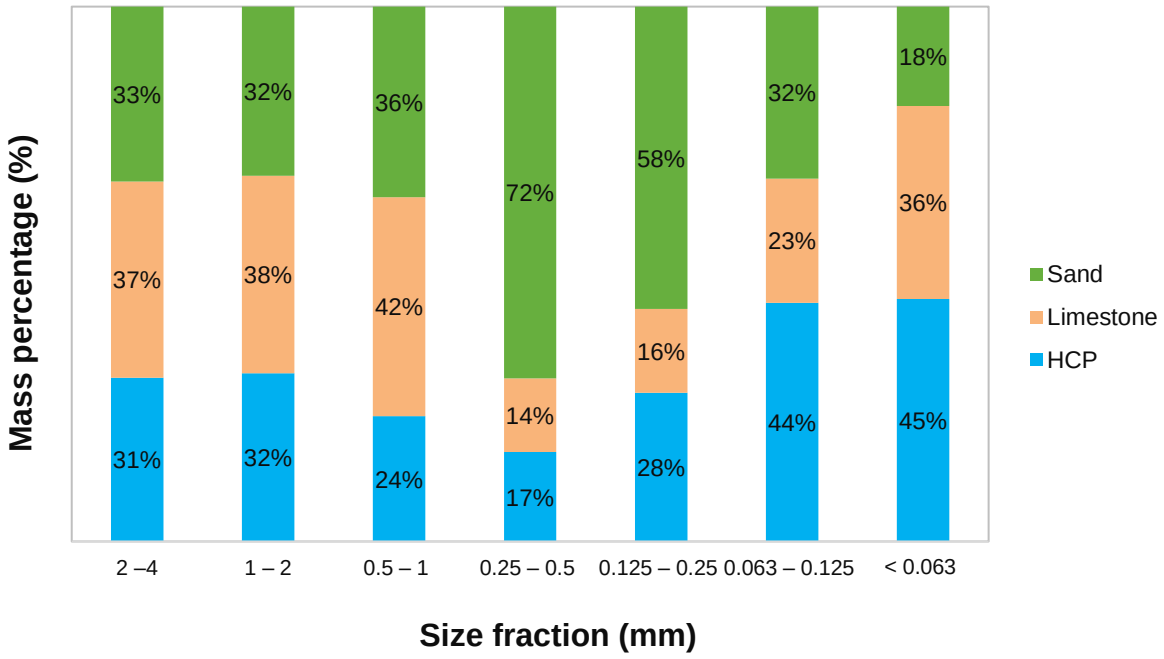

Figure 15. The barchart of mass proportions of ingredients in different size fraction of raw RCF received from MEAM (ASG/19476) after milling

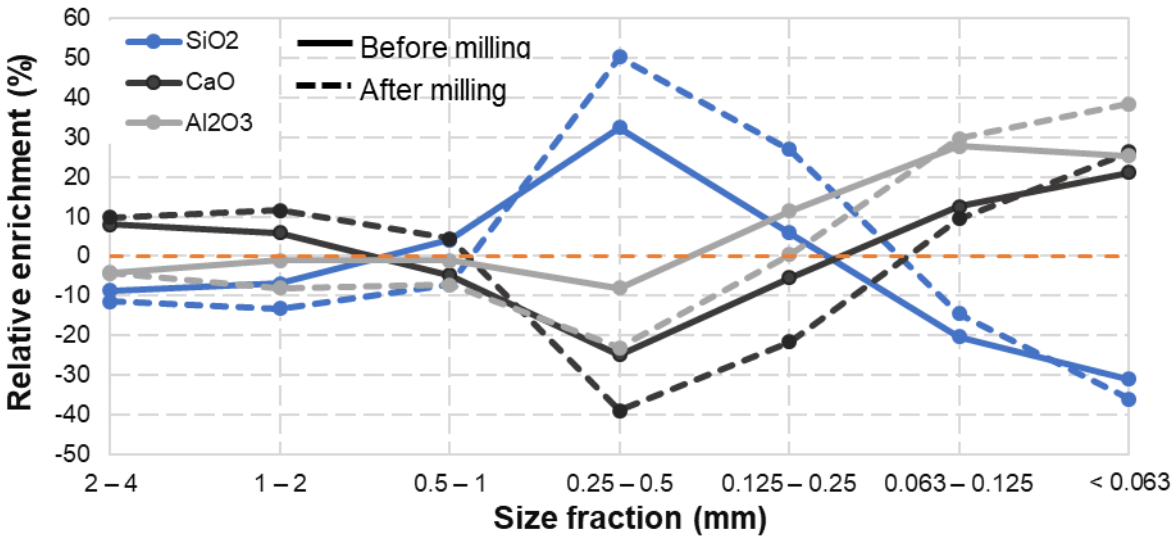

Figure 16. The relative enrichment level of the main three oxides in different size fractions of RCF

Figure 17 shows the HCP content (g/100 g of RCF) for different size fractions of raw RCF received from MEAM before and after milling. It is observed that milling has caused some drop in the HCP content of the coarse fractions (i.e., 0.25–4 mm), but the drop is not statistically significant taking into account the standard errors of each measurement plotted on the graph. There is, however, a significant in the HCP content of fine fractions (i.e., <0.125 mm). This indicates the relative effectiveness of milling in partially separating HCP from sand and transporting the HCP to the finer fractions.

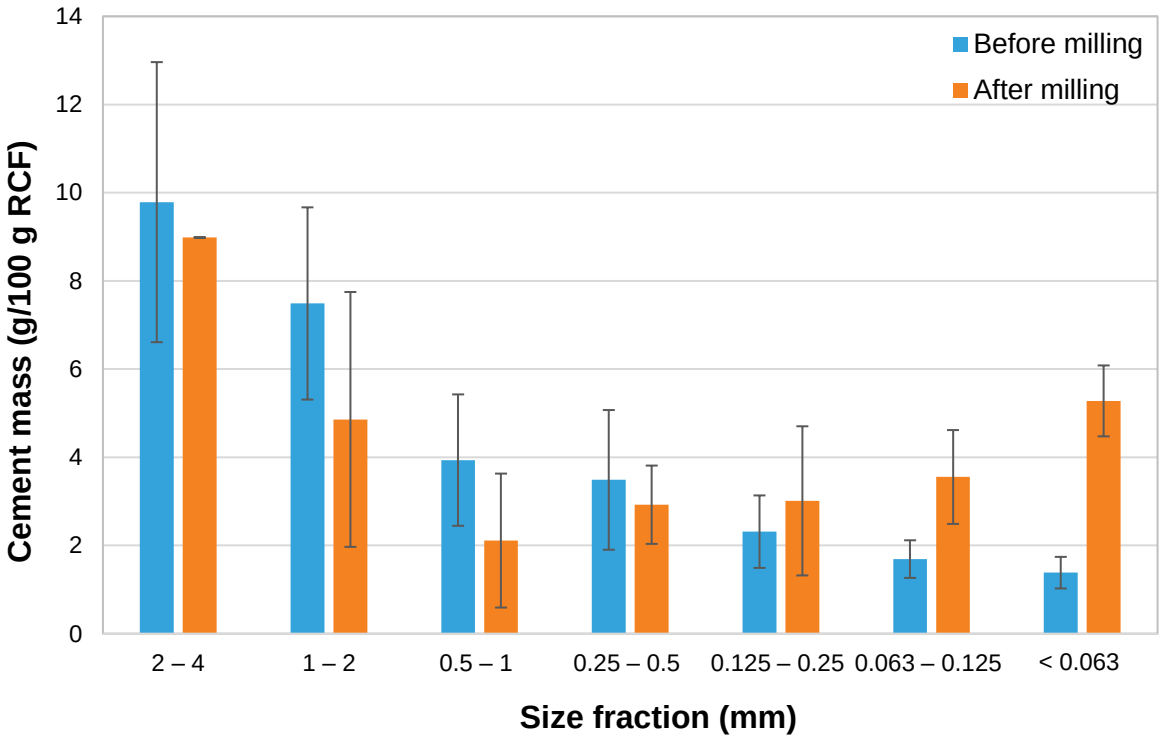

Figure 17. The cement content in different size fractions (g/100 g of RCF) for raw RCF received from MEAM before and after milling

3.6.2. MILLING BEHAVIOR AND HCP CONTENT OF RCA MICROWAVED AT 200 °C

Figure 18 shows the particle size distribution of the RCA microwaved at 200 °C (i.e., ASG/19475) before and after milling via the procedure laid out in 2.2.9. The figure at the bottom shows the individual changes in the retained values on each sieve as a cause of milling. It is observed that milling has resulted in a decrease in the retained materials on the coarser sieves (above 0.5 mm) and a growing increase on the fine sieves (i.e., 0.25 mm and below). The changes in retained fractions on each sieve is more pronounced compared to the raw RCA (ASG/19476), which could be an indication of effectiveness of microwaving in facilitating separation of HCP from aggregates. However, these results should be coupled with the HCP content analyses to be able to draw decisive conclusions.

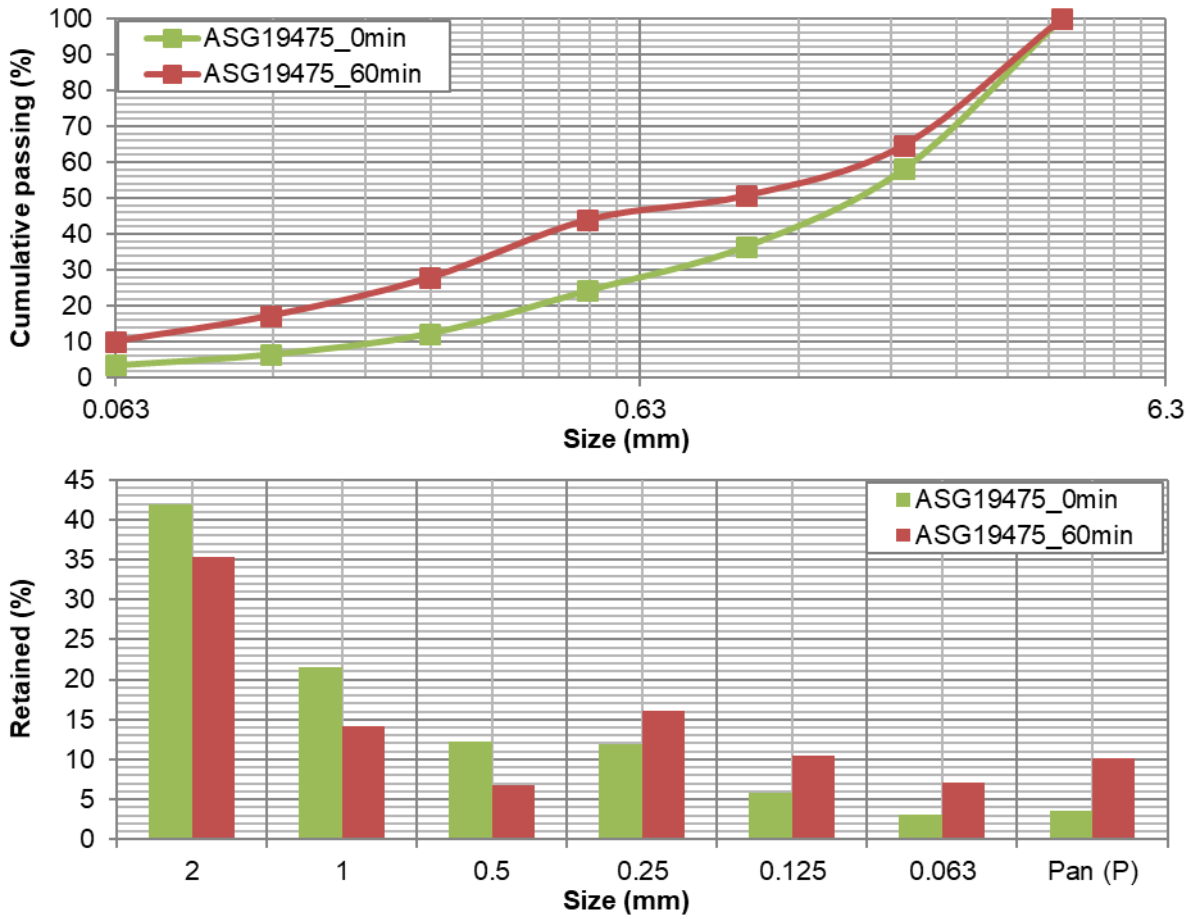

Figure 18. Particled size distribution change of RCF microwaved at 200 °C (19475) as a result of milling (top: cumulative passing; bottom: retained)

The estimation of the hydrated cement paste content on each fraction has been carried out for all size fractions of this material (both before and after milling) via the phase decomposition and bound water methods as laid out in the next section.

→ **Phase decomposition method**

Table 18 and Table 19 show the oxide composition and LOI content of different size fractions of RCF microwaved at 200 °C (ASG/19475) before and after milling, respectively. The phase decomposition method is applied on these data and the mass proportions of ingredients are estimated and shown in Figure 19 and Figure 20 for RCF microwaved at 200 °C (ASG/19475) before and after milling, respectively. It is observed that the trend of variations in the HCP content is similar to those of non-microwaved RCF (i.e., decrease in HCP as the size decreases from 4 mm to 0.5 mm, followed by increase in HCP for finer fractions). However, the mass proportion of HCP in the finer fractions of RCF after milling is relatively higher than those of RCF before milling. This is indicative of the effectiveness of milling in promoting better separation of HCP from aggregates.

Table 18. Oxide composition of different size fractions of RCF microwaved at 200 °C (ASG/19475); before milling

Oxide	Size range (mm)						
	2 – 4	1 – 2	0.5 – 1	0.25 – 0.5	0.125 – 0.25	0.063 – 0.125	< 0.063
CaO	30.8	28.4	27	22.4	29.4	33.3	33
SiO_2	38.6	42.9	46.1	55.5	43	34.5	33
Al_2O_3	3.84	4.03	4.03	3.75	4.74	5.26	5.13
Fe_2O_3	0.82	1.33	1.2	0.808	1.09	1.95	1.97
MgO	1.75	1.83	1.78	1.56	2.11	2.45	2.39
K_2O	0.425	0.375	0.315	0.536	0.47	0.438	0.492
LOI (%)	21.31	18.49	17.61	13.35	17.27	18.79	20.79

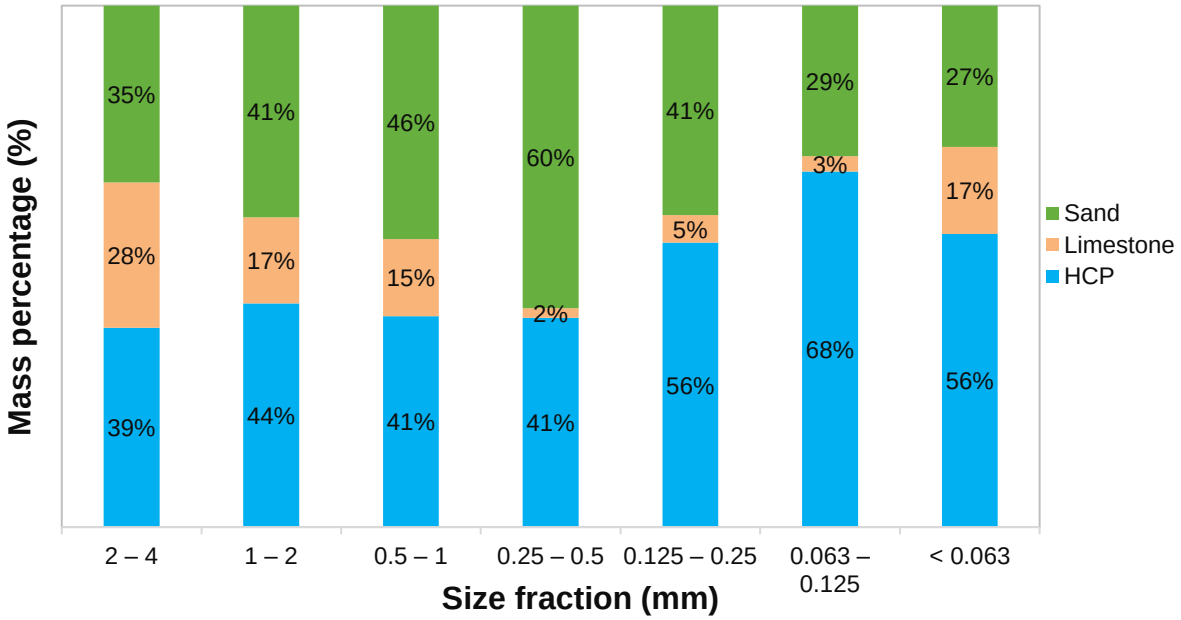

Figure 19. The barchart of mass proportions of ingredients in different size fractions of RCF microwaved at 200 °C (ASG/19475) before milling

Table 19. Oxide composition of different size fractions of RCF microwaved at 200 °C (ASG/19475); after milling

Oxide	Size range (mm)						
	2 – 4	1 – 2	0.5 – 1	0.25 – 0.5	0.125 – 0.25	0.063 – 0.125	< 0.063
CaO	31.3	31.2	29.7	16.7	25.1	34	37.5
SiO_2	38.3	38.4	41.2	66.3	50.5	33.9	28.9
Al_2O_3	3.7	3.71	3.41	2.82	4.18	5.25	5.7
Fe_2O_3	1.04	1.06	0.729	0.605	1.78	1.72	1.24
MgO	1.71	1.66	1.61	1.07	1.73	2.43	2.92
K_2O	0.3	0.265	0.349	0.488	0.562	0.382	0.308
LOI (%)	21.4	21.48	20.93	10.66	14.47	18.45	19.68

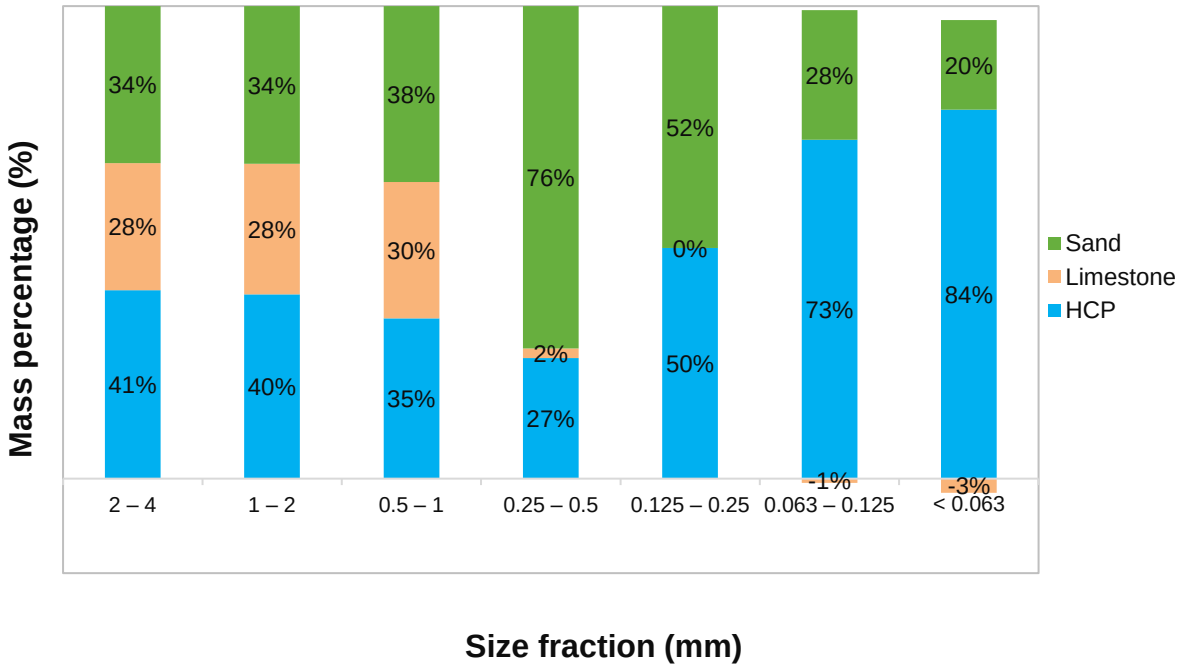

Figure 20. The barchart of mass proportions of ingredients in different size fractions of RCF microwaved at 200 °C (ASG/19475) after milling

The cement mass ratio (g/100 g of RCF) for different size fractions of RCF microwaved at 200 °C (ASG/19475) before and after milling is shown in Figure 21. It is observed that milling has resulted in a reduction in HCP content of coarse fractions (i.e., 0.5 – 2 mm) and an increase in that of finer fractions (<0.25 mm). However, the changes in HCP content as a result of milling is more pronounced compared to those of non-microwaved RCF (i.e., Figure 17), which suggests that microwaving has indeed improved the efficacy of milling in separation of HCP and sand.

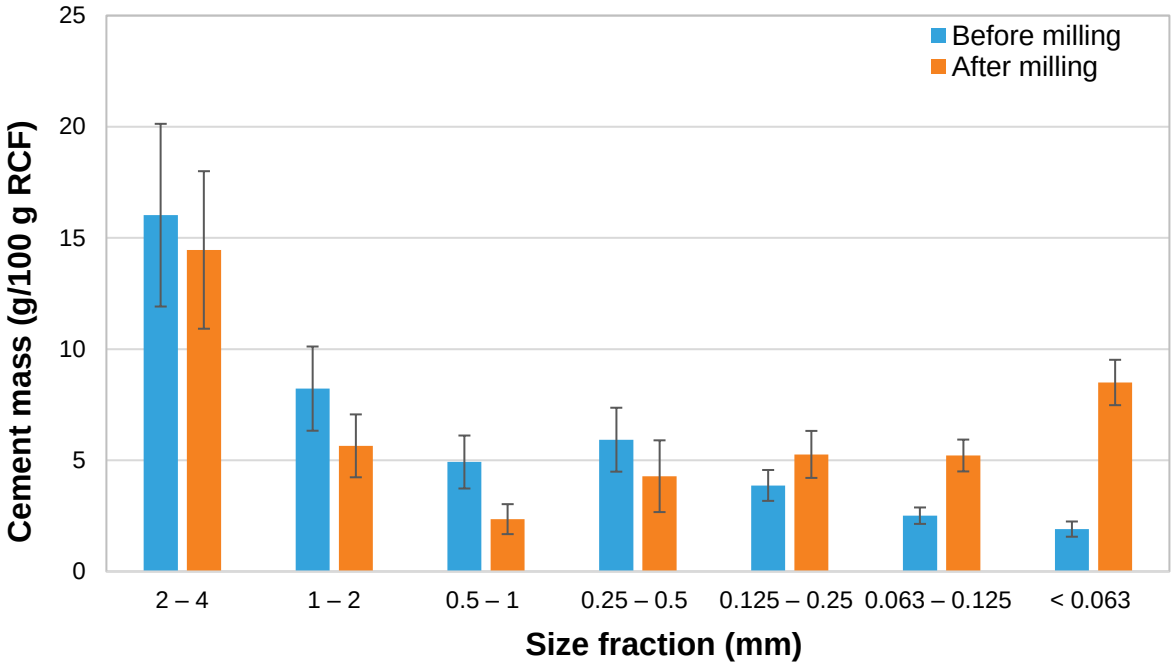

Figure 21. The cement content in different size fractions (g/100 g of RCF) for RCF microwaved at 200 °C before and after milling

→ **Bound water method**

Table 20 shows the mass loss and HCP content of each fraction of microwaved (at 200 °C) and milled RCF. Judging only by the HCP content results obtained from the bound water method, a comparison of the HCP contents of this RCF to those of non-microwaved RCF (Table 11) suggests that microwaving and milling has not led to any significant redistribution of HCP towards finer fractions. A mass balance calculation shows that this RCF (microwaved at 200°C) contains a total of 36.97% HCP, a considerably lower value compared to that of ASG/19461 (44.94%), while both come from the same concrete mixture. Part of the decrease in HCP content is most likely because of evaporation of part of bound water as a result of microwaving. Part of the evaporated water is resorbed during the rewetting cycle. However, the 17% drop in HCP estimation suggests that part of the water evaporation by microwaving is irreversible and is not negated by rewetting.

Table 20. The 550 °C mass loss (LOI) and approximate HCP content of different size fractions of RCF microwaved at 200 °C (19475) after milling

Fraction (mm)	Specimen n°	LOI at 550 °C	Approximate HCP content (%)	Average HCP content
<63µm	1	8.18	47.13	47.13%
	2	8.82	–	
63-125µm	1	10.80	62.18	62.18%
	2	8.43	–	
125-250µm	1	7.22	41.57	40.9±1.9%
	2	6.99	40.26	
250-500µm	1	5.67	32.63	34.1±4.1%

	2	6.16	35.5	
0.5-1mm	1	7.35	42.32	42.32%
	2	6.20	–	
1-2mm	1	5.72	32.95	32.95%
	2	–	–	
2-4mm	1	5.15	29.66	29.66%
	2	5.53	–	

A comparison has been made with regards to the HCP content (in %) and also the HCP mass (g/100 g of SCM) between the bound water method and phase decomposition method to assess the agreement of the two methods. Table 21 shows that there is a good agreement in the estimated values of the two methods. A linear correlation coefficient of 0.72 exists between the HCP masses and the total HCP contents estimated by the two methods are slightly different.

Table 21. The 550 °C mass loss (LOI) and approximate HCP content of different size fractions of RCF microwaved at 200 °C (19475) after milling

Method	Parameter	Size range (mm)							Sum
		2 – 4	1 – 2	0.5 – 1	0.25 – 0.5	0.125 – 0.25	0.063 – 0.125	< 0.063	
	Retaining (%)	35.30	14.09	6.72	16.07	10.53	7.13	10.16	
Phase decomposition	HCP (%)	31.33	30.65	26.84	20.19	37.87	55.63	63.76	
	Mass HCP (g/100 g RCF)	11.06	4.32	1.80	3.25	3.99	3.97	6.48	34.86
Bound water	HCP (%)	29.66	32.95	42.32	34.10	40.90	62.18	47.13	
	Mass HCP (g/100 g RCF)	10.47	4.64	2.84	5.48	4.31	4.44	4.79	36.97

3.6.3. MILLING BEHAVIOR HCP CONTENT OF RCA MICROWAVED AT 280-300 °C

Figure 22 shows the particle size distribution of the RCA microwaved at 280-300 °C (i.e., ASG/19474) before and after milling via the procedure laid out in 2.2.9. The figure at the bottom shows the individual retained values on each sieve before and after milling. It is observed that milling has resulted in a decrease in the retained materials on the coarser sieves (above 0.5 mm) and a growing increase on the fine sieves (i.e., 0.25 mm and below). Similar to the case of RCA microwaved at 200 °C (i.e., ASG/19475), the changes in retained fractions on each sieve is more pronounced compared to the raw RCA (ASG/19476), which is an indication of the effectiveness of microwaving in facilitating separation of HCP from aggregates. Furthermore, such increases are even more pronounced compared to those of RCA microwaved at 200 °C, which suggests that the microwaving temperature above 200 °C still affects the milling behavior.

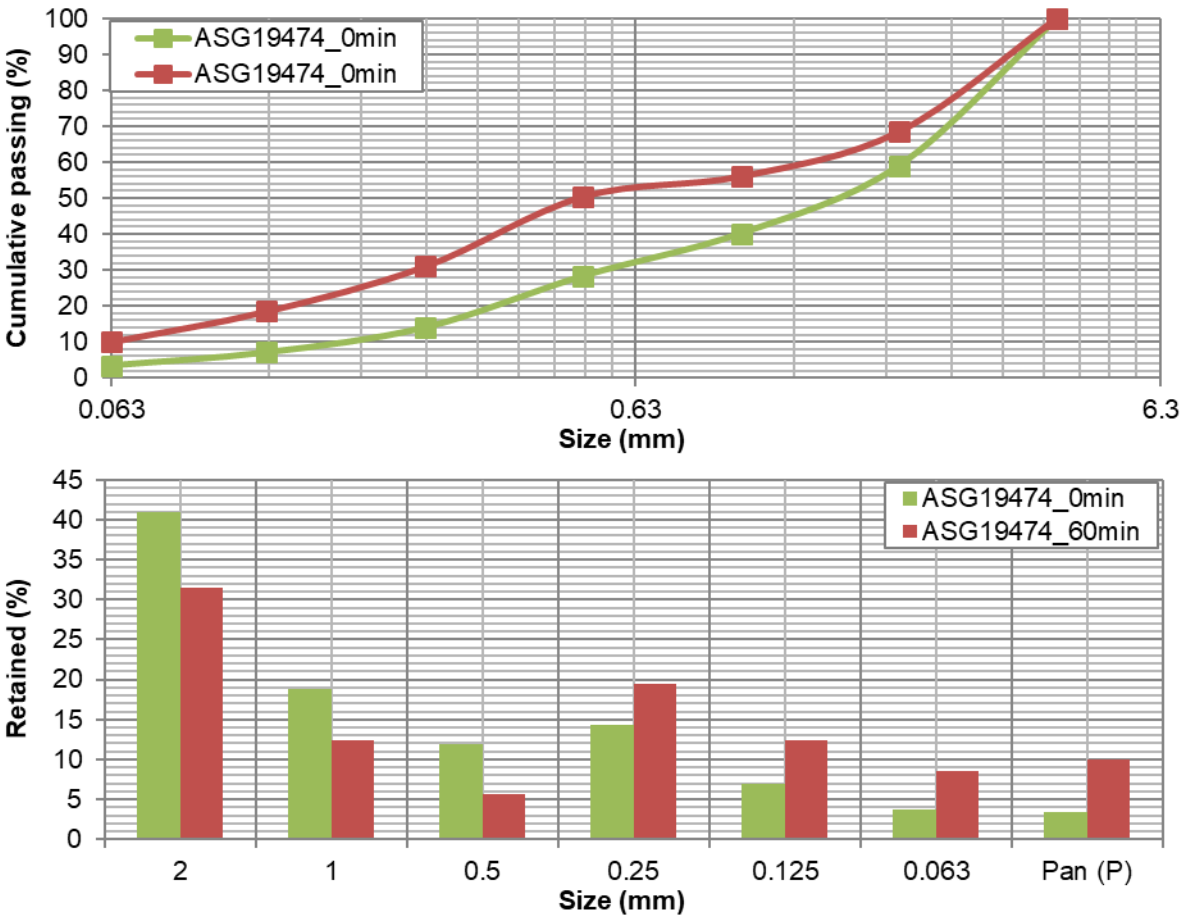

Figure 22. Particled size distribution change of RCF microwaved at 280-300 °C (19474) as a result of milling (top: cumulative passing; bottom: retained)

The estimation of the hydrated cement paste content on each fraction has been carried out for all size fractions of this material (both before and after milling) via the phase decomposition and bound water methods as laid out in the next section.

→ **Phase decomposition method**

Table 22 and Table 23 show the oxide composition and LOI content of different size fractions of RCF microwaved at 280–300 °C (ASG/19474) before and after milling, respectively. The phase decomposition method is applied on these data and the mass proportions of ingredients are estimated and shown in Figure 23 and Figure 24 for this material before and after milling, respectively. It is observed that the trend of variations in the HCP content is similar to those of non-microwaved and microwaved RCF (i.e., decrease in HCP content with decrease in size from 4 mm to 0.5 mm, followed by increase for finer fractions). However, the mass proportions of HCP in the finer fractions of RCF after milling is considerably higher than those of RCF before milling. The increase is even more pronounced than what was observed for the RCF microwaved at 200 °C. This is indicative of the effectiveness of milling in promoting better separation of HCP from aggregates and also the influence of microwaving temperature on the extent of separation.

Table 22. Oxide composition of different size fractions of RCF microwaved at 280–300 °C (ASG/19474); before milling

	Size range (mm)						
Parameter	2 – 4	1 – 2	0.5 – 1	0.25 – 0.5	0.125 – 0.25	0.063 – 0.125	< 0.063
CaO	30.6	29.6	26.9	19.7	28.1	35.3	35.4
SiO2	39.1	42.4	47.8	60.2	45.4	32.9	31.4
Al2O3	3.68	3.87	3.86	3.6	4.92	5.69	5.55
Fe2O3	1.03	0.792	0.832	1.7	1.58	1.21	1.38
MgO	1.7	1.76	1.77	1.36	2.15	2.65	2.6
K2O	0.303	0.313	0.388	0.485	0.443	0.408	0.343
LOI(%)	21.03	19.78	17.01	11.35	15.63	18.6	19.71

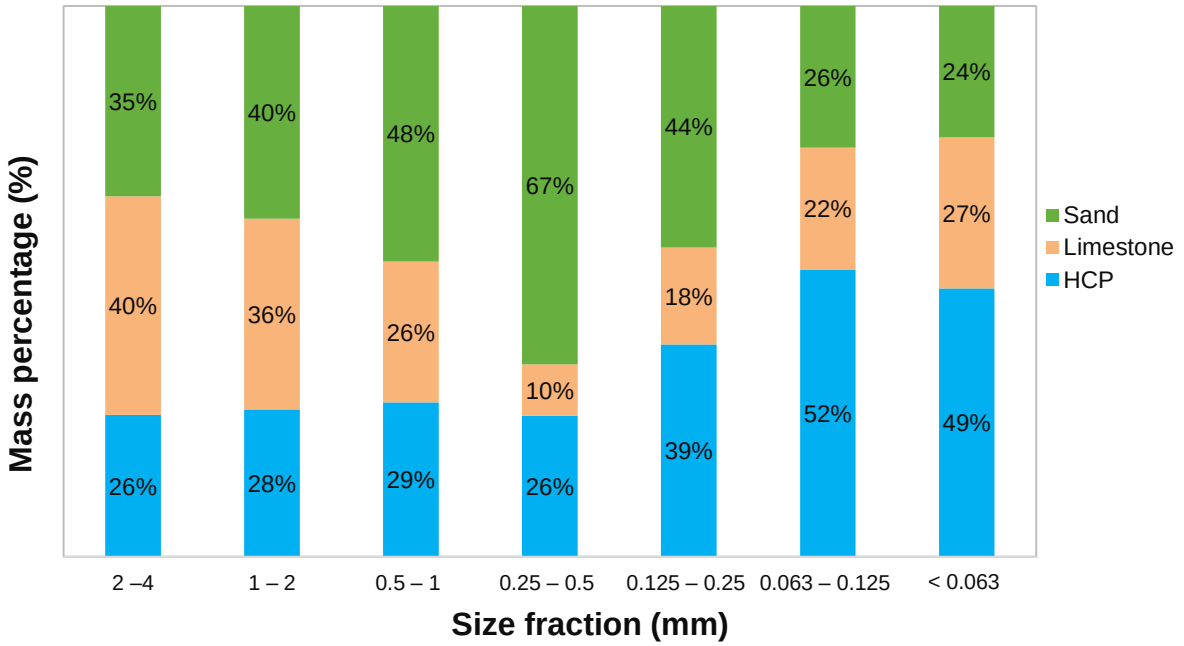

Figure 23. The barchart of mass proportions of ingredients in different size fraction of RCF microwaved at 280–300 °C (ASG/19474) before milling

Table 23. Oxide composition of different size fractions of RCF microwaved at 280–300 °C (ASG/19474); after milling

	Size range (mm)						
Parameter	2 – 4	1 – 2	0.5 – 1	0.25 – 0.5	0.125 – 0.25	0.063 – 0.125	< 0.063
CaO	33.2	32.2	30.2	13.9	22.6	35.2	37.9
SiO2	34.4	35.9	39.9	70.7	55.4	33.5	27.9
Al2O3	3.51	3.5	3.26	2.39	4.31	5.59	6.07
Fe2O3	0.683	0.7	1.21	1.08	0.827	1.17	1.75
MgO	1.6	1.67	1.55	2.015	1.63	2.65	2.99

K2O	0.332	0.324	0.28	0.389	0.56	0.437	0.299
LOI(%)	24.06	23.4	21.25	9.25	13.29	17.83	18.74

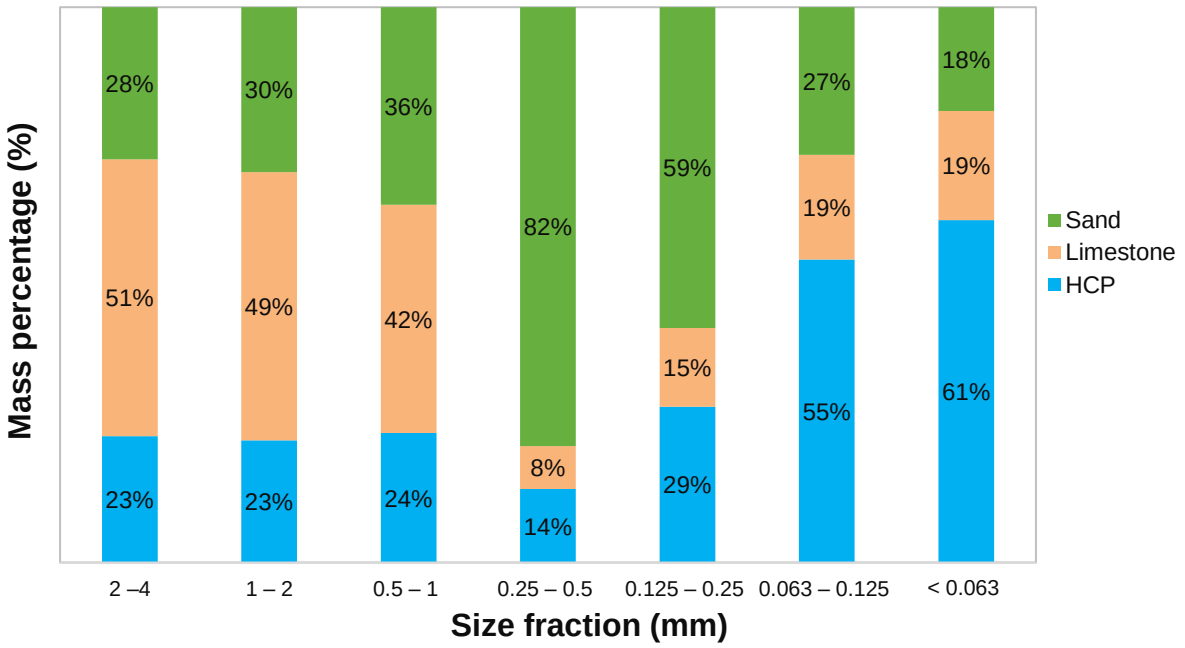

Figure 24. The barchart of mass proportions of ingredients in different size fraction of raw RCF microwaved at 280–300 °C (ASG/19474) after milling

The cement mass ratio (g/100 g of RCF) for different size fractions before and after milling is shown in Figure 25. It is observed that milling has resulted in some reduction in HCP contents of coarse fractions, but in most cases the change is not statistically significant considering the error bars shown on the plot. Significant increases are however observed in the HCP contents of the finer fractions (<0.125 mm). The intensity of changes in HCP content as a result of milling is more pronounced compared to those of RCF microwaved at 200 °C which indicates the importance of microwaving temperature in the extent of separation.

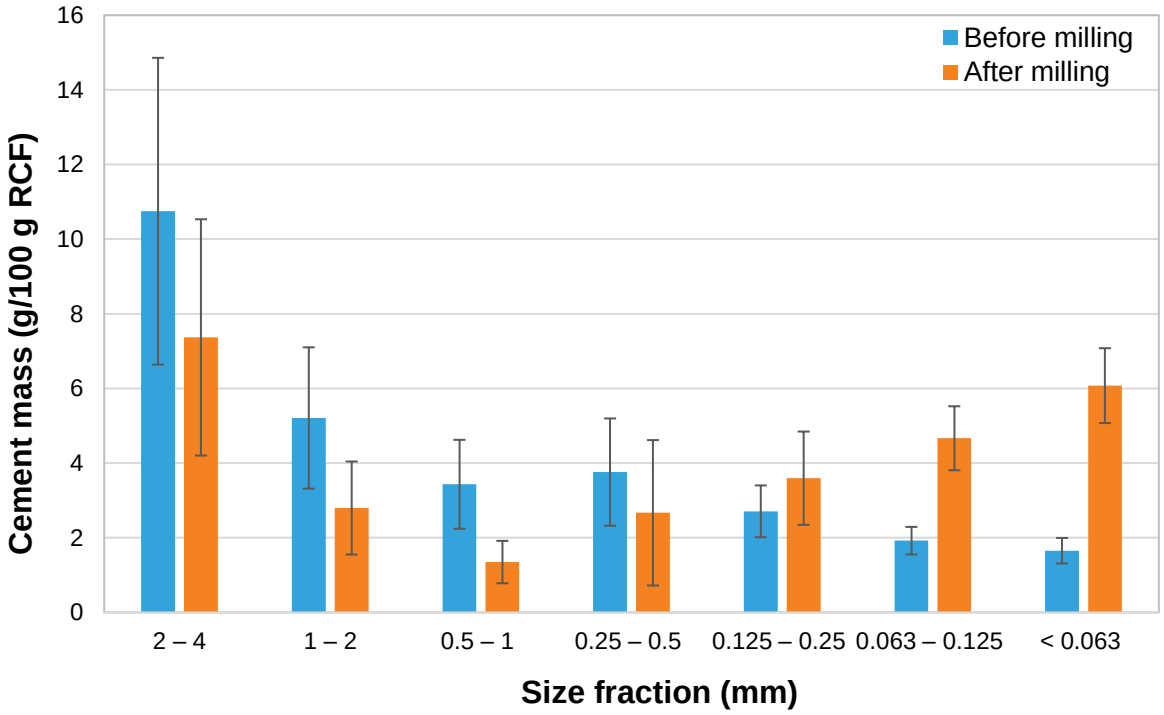

Figure 25. The cement content in different size fractions (g/100 g of RCF) for RCF microwaved at 280–300 °C before and after milling

→ **Bound water method**

Table 24 shows the mass loss and HCP content of each fraction of microwaved (at 280-300 °C) and milled RCF after milling. Comparing the HCP content results of this RCF to those of non-microwaved RCF (Table 11), it could be argued that microwaving and milling has not led to any significant redistribution of HCP towards finer fractions. A mass balance calculation shows that this RCF (microwaved at 280-300 °C) contains a total of 34.88% HCP, a considerably lower value compared to that of ASG/19461 (44.94%), while both come from the same concrete mixture. A decrease of approximately 22% in the HCP content has occurred as a result of microwaving, which could partly be due to the partial evaporation of cound water, similar to the case of RCF microwaved at 200 °C.

Table 24. The 550 °C mass loss (LOI) and approximate HCP content of different size fractions of RCF microwaved at 280–300 °C (19474) after milling

Fraction (mm)	Specimen n°	LOI at 550 °C	Approximate HCP content (%)	Average HCP content
<63µm	1	8.92	51.37	51.37%
	2	–	–	
63-125µm	1	8.20	47.23	47.23%
	2	7.76	–	
125-250µm	1	7.43	42.81	42±2.3%
	2	7.16	41.21	
250-500µm	1	5.42	31.21	28.1±8.8%

	2	4.34	24.98	
0.5-1mm	1	5.00	28.8	26.3±7%
	2	4.14	23.85	
1-2mm	1	6.11	35.17	33.4±5%
	2	5.49	31.65	
2-4mm	1	4.80	27.63	29.8±6.2%
	2	5.56	32	

A comparison has been made with regards to the HCP content (in %) and also the HCP mass (g/100 g of SCM) between the bound water method and phase decomposition methods to assess the agreement of the two methods. Table 27 shows that there is a good agreement in the estimated values of the two methods. A linear correlation coefficient of 0.91 exists between the HCP masses and the total HCP contents estimated by the two methods are slightly different.

Table 25. The 550 °C mass loss (LOI) and approximate HCP content of different size fractions of RCF microwaved at 280 °C (19474) <u>after</u> milling

Method	Parameter	Size range (mm)							Sum
		2 – 4	1 – 2	0.5 – 1	0.25 – 0.5	0.125 – 0.25	0.063 – 0.125	< 0.063	
	Retaining (%)	31.53	12.42	5.66	19.41	12.46	8.54	9.99	
Phase decomposition	HCP (%)	23.99	23.12	24.42	13.83	29.32	55.66	61.98	
	Mass HCP (g/100 g RCF)	7.56	2.87	1.38	2.68	3.65	4.75	6.19	29.10
Bound water	HCP (%)	29.80	33.40	26.30	28.10	42.00	47.23	51.37	
	Mass HCP (g/100 g RCF)	9.40	4.15	1.49	5.45	5.23	4.03	5.13	34.88

3.6.4. COMPARISON OF THE EFFECTIVENESS OF MICROWAVING IN THE TRANSPORTATION OF HCP TOWARDS FINER FRACTIONS

The HCP contents (in g/100 g SCM) are plotted for the non-microwaved and microwaved RCFs before milling (Figure 26) and also after milling (Figure 27). It is observed that the cement masses constantly decrease with decrease in size fraction and the differences in the cement content of different fractions are not significant. Comparing Figure 26 to Figure 27 reveals that milling causes considerable change in the distribution of HCP in different fractions. However, the differences between the raw and microwaved fractions (although visible) are not very significant compared to the standard errors.

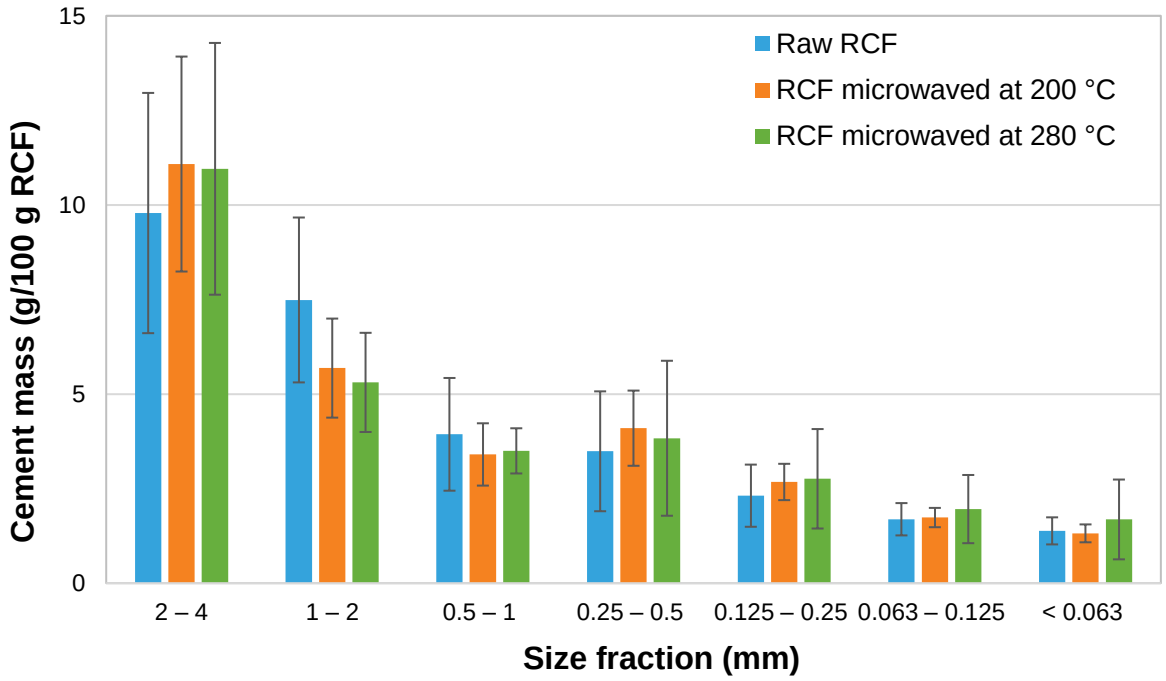

Figure 26. The HCP content in different size fractions (g/100 g of RCF) for raw and microwaved RCF before milling

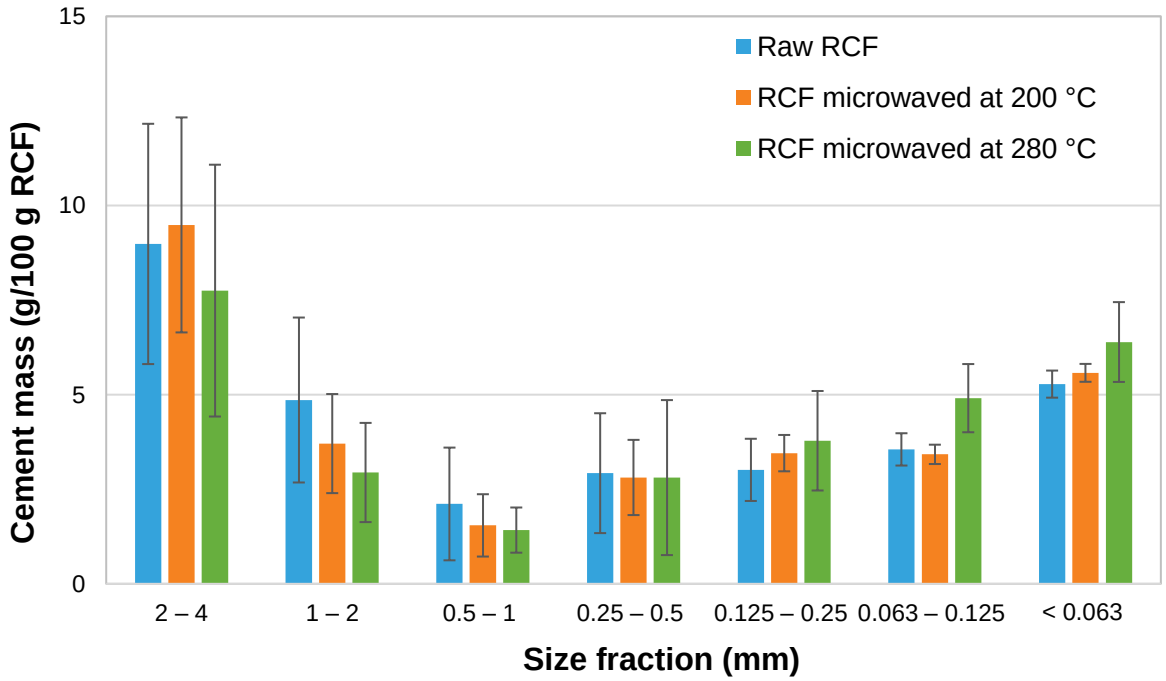

Figure 27. The HCP content in different size fractions (g/100 g of RCF) for raw and microwaved RCF after milling

3.7. CHARACTERIZATION OF THE RCA AND RCF SENT BY GBN/MEAM TO VITO

3.7.1. WATER ABSORPTION

The 7th batch of materials sent to VITO for characterization are listed in Table 1 under row 7. The water absorption of GBN Coarse 4/8_ADR was found to be 6.84%, which is considerably larger than that of raw RCCA (5.24%). This could be partially because of the smaller particle size range of this material (i.e., 4/8) than that of raw RCCA (4/16). The RCF obtained from the HAS technology has a significantly larger water absorption (WA = 15.56%) compared to those of raw or microwaved RCF received from MEAM (see Table 15). This could be partially due to the higher temperature of HAS treatment, leading to a large loss in HCP bound water, but also due to a higher content of HCP in the material. However, the phase decomposition analysis below shows that GBN 1/4_GBN contains less HCP compared to fines received from MEAM as shown below.

3.7.2. HYDRATED CEMENT PASTE CONTENT

→ Phase decomposition method

Table 26 shows the oxide composition, LOI and (indicative) density values of the RCF's received from GBN/MEAM. The results are analyzed via the developed phase decomposition method and the mass proportions of HCP, limestone and sand are estimated and plotted in Figure 28. It is observed that the HCP contents are very low, especially for fine fractions. It could thus be concluded that these RCF's are lean in HCP and not very interesting for valorization purposes. Note that the high SiO_2 content in the chemical composition justifies the high estimated values for sand.

Table 26. Oxide composition of different size fractions of RCF received from GBN/MEAM and analyzed via phase decomposition method

	HCP/19489	HCP/19490	HCP/19491	HCP/19492	HCP/19493
	GBN Coarse 4/8	GBN 0/4 HAS	GBN 0/1 ADR	GBN 0/1 HAS	MEAM-GBN HAS 0/1
CaO (%)	31.3	26.7	22.6	11.8	10.6
SiO_2 (%)	36.3	44.9	50.7	70.1	73.1
Al_2O_3 (%)	3.25	3.56	3.53	4.64	4.94
Fe_2O_3 (%)	0.659	0.801	0.845	1.42	1.42
MgO (%)	1.43	1.41	1.36	1.52	1.35
K_2O (%)	0.29	0.386	0.472	0.818	0.695
LOI (%)	24.64	19.85	18.22	7.7	5.84
Density (g/cm^3)*	2.69	2.69	2.69	2.69	2.69

* density values are indicative. As shown in Section 2.2.8 under sensitivity analysis, variations in density has almost no effect on results. As such, the measurements are skipped.

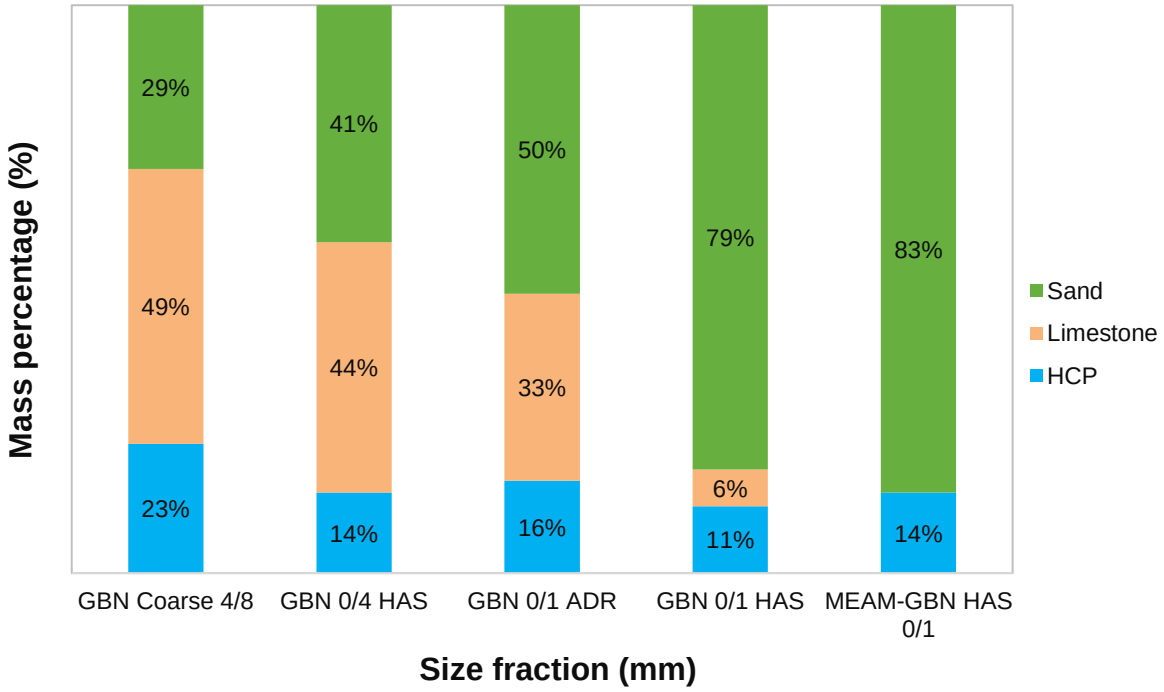

Figure 28. The barchart of mass proportions of ingredients in different size fraction of RCF received from GBN and MEAM and analyzed via phase decomposition method

Bound water method

The materials were analyzed for their bound water and HCP content. Before measuring the LOI, the materials were soaked in water for 24 h for resorption of evaporated water during heating/microwaving. Table 27 shows the loss on 550 °C ignition and the estimated HCP content for the different materials received from GBN. The coarse 4/8 fraction (i.e., GBN Coarse 4/8_ADR) showed an average of 25.5% HCP. The GBN 1/4_HAS fraction contains considerably more HCP compared to the coarse fraction (30.9%). Also the 0/1 ADR contains a high HCP content (37.7%) which might indicate even higher HCP contents for the fine fractions of this material compared to the 1/4_HAS fraction.
The 0/4 airknive microwaved at 250 °C and the 0/1 Rotor (ASG/20079 and 20080) showed very low LOI and thus the HCP estimated in both cases is outstandingly low. This could be either because the fractions indeed contain low HCP, or that resorption of water did not fully take place for these materials.

Table 27. The 550 °C mass loss (LOI) and approximate HCP content of different RCF fractions of CBS concrete microwaved at 280–300 °C (19474) after milling

Sample code	Fraction (mm)	Specimen n°	LOI at 550 °C	Approximate HCP content (%)
ASG/19489	GBN Coarse 4/8_ADR	1	5.07	29.22
ASG/19490	GBN 1/4_HAS	1	5.99	34.51

ASG/19491	GBN 0/1_ADR	1	6.66	38.36
ASG/19492	GBN 0/1 HAS	1	5.41	31.18
ASG/19493	MEAM-GBN 0/1_HAS	1	5.09	29.35
ASG/20079	0/4 Airknives Microwaved at ~250 °C	1	2.65	15.26
ASG/20080	0/1 Rotor Microwaved at ~220-250 °C	1	2.96	17.06

CHAPTER 4 CONCLUSIONS

The first three batches of crushed concrete aggregates were produced at SCC using the lab-scale Smart Crusher. The mass balance analysis suggests that this Smart Crusher produces a considerable amount of fines (<2 mm), which is not desirable for recycling purposes when compared to other methods of crushing such as a jaw crusher. The cement content in the fines produced by SCC were found to have 12 – 35% hydrated cement paste with increasing values for the finer fractions. Nonetheless, the lab-based Smart Crusher technology was deemed unsatisfactory as of now in properly crushing and recycling concrete into its constituting ingredients [1]. As such, alternative methods were contemplated within the consortium for recycling the concrete such that the aggregates, sand and cement paste are separated as much as possible.

One such method was thermal heating followed by crushing which was mainly investigated by VUB. Another alternative method was microwave-assisted crushing, where the concrete rubbles were first microwaved at MEAM at 200 to 300 °C followed by crushing using jaw crusher. The particle size distribution of the jaw crusher output among the non-microwaved and microwaved RCAs suggested that microwaving prior to crushing leads to finer RCAs and that microwaving temperature has a direct impact on fineness. This could be interpreted as the effectiveness of microwaving on better fragmentation of concrete. Although microwaving resulted in some 10% decrease in resistance against fragmentation, the coarse fractions were found to have satisfactory level of mechanical resistance and thus suitable for use in new concrete. The water absorption of the coarse and especially fine fractions of raw and microwaved RCA are still very high. Despite ~5% water absorption, it can be argued that the coarse fraction is still useful in making concrete, but the fine fraction is not recommended for such application at this point.

Preliminary examinations of microwaved, crushed RCFs suggested that microwaving alone did not result in higher proportions of hydrated cement paste (HCP) in the finer fractions. As such, milling of the RCFs after microwaving and crushing was applied to potentially pulverize the cement paste and transport it to very fine fractions for the purpose of sieving, recovery and valorization as SCM in concrete. The sieve analysis of the RCFs before and after milling suggests a decline in the overall mass retaining on coarser fractions and increase in those of finer fractions. Phase decomposition analysis of microwaved and raw RCFs before and after milling clearly indicate that milling can partly transport the HCP from coarses fractions towards finer fractions. Moreover, microwaving can further facilitate this process as higher microwaving temperatures (e.g., 200 °C vs 300 °C) were found to undergo more separation of HCP and sand.

The coarse and fine fraction outputs of GBN ADR-HAS technology were also tested for their water absorption and LOI at 550 °C after rewetting. The results suggest that the GBN outputs generally have a higher water absorption (which could be due to the evaporation of part of the bound water of HCP during the HAS combustion period, which is then partially resorbed during water absorption test and resulted in a inflation in this parameter: WA). Also, the LOI results do not suggest any advantage of GBN outputs in terms of HCP content compared to fractions produced by jaw crusher. Finally, with regards to the mechanical performance of the coarse fraction, the results suggest that the coarse RCA output of all methods have satisfactory mechanical performance (as per LA factor).

[1] Recently, unconfirmed results by Smart Crusher suggests that the industrial scale machine might indeed be able to separate the aggregates from the hydrated cement paste. A crushing campaign is thus being scheduled for assessing the performance of the smart crusher.

REFERENCES

1. *BS EN 933-1:2012. Tests for geometrical properties of aggregates. Determination of particle size distribution. Sieving method.*
2. *BS EN 1097-6:2013. Tests for mechanical and physical properties of aggregates. Determination of particle density and water absorption.*
3. *BS EN 1097-2:2010. Tests for mechanical and physical properties of aggregates. Methods for the determination of resistance to fragmentation.*
4. *BS EN 1097-1:2011. Tests for mechanical and physical properties of aggregates. Determination of the resistance to wear (micro-Deval).*
5. *BS EN 206-1:2000. Concrete. Specification, performance, production and conformity.*
6. Etxeberria, M., et al., *Influence of amount of recycled coarse aggregates and production process on properties of recycled aggregate concrete.* Cem. Concr. Res., 2007. **37**: p. 735-742.
7. Corinaldesi, V., *Mechanical and elastic behaviour of concretes made of recycled-concrete coarse aggregates.* Constr. Build. Mater., 2010. **24**: p. 1616-1620.
8. Silva, R.V., J. de Brito, and R.K. Dhir, *Fresh-state performance of recycled aggregate concrete: A review.* constr. Build. Mater., 2018. **178**: p. 19-31.
9. Zhao, Z., et al., *Influence of hardened cement paste content on the water absorption of fine recycled concrete aggregates.* Journal of Sustainable Cement-Based Materials, 2013. **2**: p. 3-4.
10. 121-DRG., R., *Specifications for concrete with recycled aggregates.* Materials and Structures, 1994. **27**(9): p. 557-559.